Summer 2017

Regulation of the Odorant Receptor ODR-10 via Endoplasmic Reticulum-Associated Degradation in Caenorhabditis elegans

Alexandra Townsend
Western Washington University, townsea3@wwu.edu

REGULATION OF THE ODORANT RECEPTOR ODR-10 VIA ENDOPLASMIC RETICULUM-ASSOCIATED DEGRADATION IN CAENORHABDITIS ELEGANS

By

Alexandra Townsend

Accepted in Partial Completion
of the Requirements for the Degree
Master of Science

Kathleen L. Kitto, Dean of the Graduate School

ADVISORY COMMITTEE

Chair, Dr. Caroline Dahlberg

Dr. David Leaf

Dr. Jacqueline Rose

MASTER'S THESIS

In presenting this thesis in partial fulfillment of the requirements for a master's degree at Western Washington University, I grant to Western Washington University the non-exclusive royalty-free right to archive, reproduce, distribute, and display the thesis in any and all forms, including electronic format, via any digital library mechanisms maintained by WWU.

I represent and warrant this is my original work, and does not infringe or violate any rights of others. I warrant that I have obtained written permissions from the owner of any third party copyrighted material included in these files.

I acknowledge that I retain ownership rights to the copyright of this work, including but not limited to the right to use all or part of this work in future works, such as articles or books.

Library users are granted permission for individual, research and non-commercial reproduction of this work for educational purposes only. Any further digital posting of this document requires specific permission from the author.

Any copying or publication of this thesis for commercial purposes, or for financial gain, is not allowed without my written permission.

Alexandra Townsend
July 20, 2017

REGULATION OF THE ODORANT RECEPTOR ODR-10 VIA ENDOPLASMIC RETICULUM-ASSOCIATED DEGRADATION IN CAENORHABDITIS ELEGANS

A Thesis
Presented to
The Faculty of
Western Washington University

In Partial Fulfillment
Of the Requirements for the Degree
Master of Science

by
Alexandra Townsend
July 2017

ABSTRACT

The study of protein degradation mechanisms in neurons can advance our understanding of multiple neurodegenerative diseases, such as Alzheimer's and Parkinson's disease. Endoplasmic reticulum-associated degradation (ERAD), plays an important role in reducing ER stress by degrading accumulating misfolded proteins, which in turn prevents cell death. Many proteins involved in ERAD are known, but the mechanisms themselves and roles of the proteins are not yet fully understood. We use the nematode *Caenorhabditis elegans* as a model for studying ERAD mechanisms. In particular our research focuses on the ubiquitin-proteasome system (UPS) in ERAD. Ubiquitin-proteasome systems have the ability to modify proteins and target them for degradation. Our goal is to help determine the relationship of the E2 and E3 ligase proteins of ERAD in neurons by studying the regulation of the transmembrane olfactory receptor ODR-10, in the AWA neurons of *C. elegans*. The ubiquitin pathway in ERAD involves multiple ubiquitin ligases (E2s and E3s). The interactions between the E2 and E3 enzymes, and their target specificity in the endoplasmic reticulum is not well understood in metazoan systems. Our research highlights the role and interactions of the E2 and E3 proteins with regards to regulation of ODR-10. We have analyzed the effects of loss of function mutations of E2 and E3 proteins to determine their effects on localization, expression levels of ODR-10, and also behavioral changes. Based upon this data we can make inferences of potential E2 and E3 protein interactions. Researching ODR-10 ubiquitin regulation in ERAD will enable us to further understand protein regulation in neurons. Through characterizing pathways that reduce cell stress, such as ERAD, we may even gain insight as to potential limits or treatments of neurodegenerative diseases.

ACKNOWLEDGEMENTS

I would like to acknowledge my thesis advisor Dr. Lina Dahlberg, and my committee members Dr. David Leaf and Dr. Jackie Rose for their guidance and knowledge. I would also like to acknowledge the Biology Department for funding my master's degree and research through the Biology Alumni Fellowship and Biology Faculty Fellowship. I would like to thank Western Washington University and the Biology Department for providing me a teaching assistantship position, which paid for my tuition and provided a stipend for myself. These funds allowed me to focus on my thesis and Master's education. I would like to acknowledge the undergraduates in the lab that have helped with my project, Sam Witus, Ellen Zocher, Nelson Ruth, Marissa Hogg, and Sam Reardon, in assisting with perpetuating worms, backcrossing mutants, creating plates, and assisting in transformations. Without their help I would not have accomplished as many projects as I wanted to complete. I would also like to acknowledge Dr. Ben Miner for his assistance with the program R to analyze data and create box and whisker plots for chemotaxis data. I would like to acknowledge the Klevit Lab of the University of Washington, in particular Tobias Ritterhoff, for providing insight into the structure of the E2 proteins and which point mutations most likely cause loss of function. The Ailion lab for allowing us to use their injection station to create transgenic animals. The CGC and MMP project for providing us with the mutant strains we used in this study. Most of all, I would like to acknowledge my family and my fiancé, Kyle Cheney, for standing by my side and providing emotional and financial support throughout my educational journey.

TABLE OF CONTENTS

LIST OF TABLES

LIST OF FIGURES

INTRODUCTION

Understanding normal cellular function in neurons will provide information about what may be happening in at-risk individuals of neurodegenerative diseases. In particular, a clearer understanding of protein degradation pathways, will allow us to further analyze causes for diseases and define possible treatments. For instance, protein aggregation is known to lead to a number of neurodegenerative disorders and other genetic diseases, such as Alzheimer's and Parkinson's (Mittal et al., 2015). The cause of protein aggregation within neurodegenerative diseases is not yet fully understood. Therefore, studying pathways that regulate protein aggregation and reducing cell stress will be important in depicting what may be the underlying causes to neurodegenerative disorders. As cells differentiate and specialize, a large volume of specific proteins is necessary to carry out various functions. Protein and RNA alone can take up as much as 40% of a cell's entire volume (Mittal et al., 2015). With such high density, proteins must maintain abundance within specific ranges to avoid overcrowding and potential protein aggregation. If protein production and degradation are not balanced they cause cellular stress, which can result in cell death and onset of neurodegeneration (Lee et al., 2015).

The secretory pathway and UPS

The ubiquitin-proteasome system (UPS), plays an important role in neurodegeneration and regulating protein aggregation. When proteins involved in the UPS do not function properly, they no longer regulate protein levels in neuronal cells and trigger cell death (Chung et al., 2001). One pathway that requires close protein production regulation by the UPS is the secretory

pathway. In mammals an estimated one third of the genome encodes proteins destined for the secretory pathway (Olzmann et al., 2013). The secretory pathway processes all proteins that will be secreted from the cell or reside in the plasma membrane. During translation, transmembrane or secretory proteins are transported to the endoplasmic reticulum (ER), then after completion of translation and proper folding they are trafficked to the Golgi apparatus and ultimately are exported to their final destinations (Cooper, 2000).

Within the secretory pathway, the UPS regulates protein degradation at the ER since this organelle is one of the first to come into contact with misfolded or damaged proteins. The ER serves as the primary gateway for the secretory pathway (Fewell et al., 2001). The main functions of the ER are facilitating disulfide bond formation and ensuring proper topology during protein folding (Fewell et al., 2001). This sizeable role requires the ER's processing of proteins to be highly regulated to ensure that the cell produces fully functional proteins at the necessary levels. Before proteins are transported to the Golgi, multiple check points for misfolded, damaged, and incomplete proteins are performed, this is known as ER quality control (ERQC) (Vembar and Brodsky, 2008). In the ER lumen, a chaperone protein, BiP, binds to newly translated polypeptides and chaperones the proper folding of the hydrophobic regions of proteins (Rutledge et al., 2009). As part of regulation, BiP remains attached to improperly folded hydrophobic regions and either retains them within the ER lumen or they are subsequently degraded via ER stress response pathways (Cooper, 2000; Rutledge et al., 2009). This mechanism prevents non-functional proteins from advancing through the secretory pathway, which is considered toxic to the cell and can cause cell death.

ER quality control

The two main mechanisms that collaborate in response to protein quality control at the ER, the unfolded protein response (UPR) and endoplasmic reticulum-associated degradation (ERAD), reduce ER stress and prevent cell death. The UPR is induced by aggregation of misfolded or unassembled proteins within the ER lumen (Cao and Kaufman, 2012). The UPR has distinct pathways relatively conserved among metazoans (Moore and Hollien, 2012). In response to BiP's remaining bound to misfolded proteins, the UPR initiates transcriptional upregulatory and translational inhibitory mechanisms in an attempt to balance the amount of protein degradation with the amount of protein production. Genes transcriptionally upregulated by the UPR encode proteins that degrade mRNA localized at the ER to reduce translation (Hollien and Weissman, 2006). With widespread translational inhibition, the uptake of polypeptides into the ER lumen is also reduced (Harding et al., 2000). By inhibiting translation and reducing the abundance of many mRNAs, the cell is able to manage the aggregated proteins already accumulated within the ER without adding more protein to the cellular environment. The UPR also upregulates transcriptional activation of genes involved in the secretory pathway and protein degradation (Travers et al., 2000). By upregulating these proteins, the cell is able to increase the processing and degradation of the proteins accumulated within the ER, reducing stress.

ER-associated degradation (ERAD) is the second response that can occur from ER stress and is the mechanism our study is focused upon (Figure1). Some genes associated with ERAD are also transcriptionally activated through mechanisms involved in the unfolded protein response (Travers et al., 2000). However, ERAD is capable of ensuring homoeostasis without the

involvement of UPR (Shen et al., 2004). The ERAD pathway removes and induces degradation of misfolded and unassembled proteins from the ER into the cytoplasm (Vembar and Brodsky, 2008). Once the targeted substrates are retained in the ER lumen by BiP, a number of proteins direct the substrate target to the ER membrane to be retrotranslocated, or removed from the ER lumen into the cytoplasm. The protein p97, also known as the velosin containing peptide (VCP), is responsible for ATP-dependent retrotranslocation and interacts with the ubiquitin-proteasome system pathway of ERAD (Ye et al., 2005).

The ubiquitin-proteasome system of ERAD

Once misfolded proteins are at the membrane of the ER, E2 ubiquitin ligases and E3 ubiquitin ligases residing in the ER membrane mark the proteins for degradation via the ubiquitin-proteasome system. Ubiquitination occurs in a four step process and often results in recognition for degradation by the 26S proteasome in the cytosol (Ciechanover and Masucci, 2002; Papaevgeniou and Chondrogianni, 2014). 1) The E1 ubiquitin activating enzyme adenylates the C-terminal glycine residue in ubiquitin, in turn "activating" the glycine residue. The E1 protein then binds to the activated glycine protein by forming a thioester bond with the catalytic cysteine site of the E1 protein. 2) E1 proteins then transfer the activated ubiquitin to ubiquitin carrying E2 ligases, which create another thioester bond with the glycine in the activated ubiquitin by a conserved catalytic cysteine in the E2 protein. 3) The E2 protein then binds to an E3 ubiquitin protein ligase that is bound to the targeted substrate of interest. E2 proteins then modify the substrate with ubiquitin while the substrate is still bound to the E3 ligase. The ubiquitin modifier if covalently linked via its C-terminal glycine residue to a lysine

residue on the substrate forming an isopeptide bond. 4) This cycle is repeated, linking ubiquitin to lysines on the previously added ubiquitin to create a polyubiquitin chain on the substrate protein. Depending on the number of ubiquitin molecules and their location on a target substrate, adaptor proteins associated with the 26S proteasome in the cytoplasm recognize the protein as marked for degradation.

There are dedicated E3 ligases and E2 proteins for ERAD, which have been, to date, primarily studied in yeast. Genetic and biochemical analyses identify two pathways, involving different E3 ligase proteins, which carry out substrate targeting. One involves the E3 ligase Hrd1 (HRD-1 is a homolog and HRDL-1 is a paralog in *C. elegans*), which resides within the ER membrane and catalyzes ubiquitination of ERAD substrates in the ER lumen and ER membrane (Sasagawa et al., 2007). The other is a complex containing the Doa10 E3 ligase (the *C. elegans* ortholog is MARC-6), which also resides in the ER membrane and catalyzes ubiquitination of ERAD substrates in the cytosol and nucleoplasm (Deng and Hochstrasser, 2006). Doa10 also targets some ER transmembrane proteins as well (Habeck et al., 2015; Zattas et al., 2016). The E2 proteins associated with the three E3 ligases in ERAD are known, and in some cases have specific to which E3 ligases with which they interact. The E2 protein Ubc7 associates with E3 ligases Doa10 and Hrd1 (Cohen et al., 2015). Hrd1 also associates with E2 protein Ubc6 (Araki and Nagata, 2011). The E3 ligase HRDL-1, in *C. elegans*, interacts with E2 protein UBC-6 (Hirsch et al., 2009). These E2 proteins bind to the appropriate E3 ligase and polyubiquitinate the target substrate. Once ubiquitinated, ERAD substrates are recognized and degraded in the cytoplasm by the 26S proteasome. Further research will determine if this pathway is also represented in multicellular organisms, such as *C. elegans* and mammals.

Another more recent yeast biochemical analysis provides insight to a different ubiquitin pathway in ERAD. In this case, the E2 proteins, Ubc6 and Ubc7, work in tandem to create the ubiquitin chain on a target substrate. Ubc6 first binds to the E3 ligase-target substrate complex and attaches the first ubiquitin (Weber et al., 2016). Then, Ubc7 binds to the E3 ligase-target substrate complex and polyubiquitinates the target substrate, creating the ubiquitin chain (Weber et al., 2016). Finally, once the target substrate is polyubiquitinated at the ER membrane, it is moved into the cytoplasm where it can be degraded by the 26S proteasome.

Biochemical analyses in yeast provide clues as to how the ubiquitin pathway regulates misfolded proteins within ERAD. The question remains if the E2 proteins are specific for which E3 ligase they can interact with, if they work in tandem and interact with all E3 ligases, or if a combination of both mechanisms exists. Our interest is in determining if these mechanisms are also present within multicellular organisms, in which there are few studies. Human homologs of the E2 and E3 ligase proteins have been identified, but it is unknown if these homologs function in the same manner as their yeast counterparts (Burr et al., 2011; Sasagawa et al., 2007). The E3 ligases in yeast are specific for what they target in terms of luminal vs. cytoplasmic substrates (Huyer et al., 2004). However, it is not understood how, and if, all substrates are selectively targeted and if chaperone proteins are always involved as seen by some substrates targeted by Doa10 in yeast (Huyer et al., 2004; Shiber et al., 2013). There are situations where substrates are targeted by both E3 ligases in yeast and the E3 ligases do not show specific selectivity (Huyer et al., 2004).

Yeast is a unicellular organism, and these studies can only provide insight into how ERAD functions in individual, uniform cells. In multicellular organisms, it is not fully understood if ERAD functions the same in all cell types or if expression of E2 and E3 ligase

proteins varies from cell to cell. Multicellular organisms also tend to have more E2 and E3 ligase proteins involved in ERAD than yeast (Sasagawa et al., 2007; Tamura et al., 2010). Very little is known about the ERAD mechanism in neurons of multicellular organisms and if the E3 ligases display similar selective targeting of sensory receptors. Multicellular organisms also contain more E3 ligases and E2 proteins than yeast, so these proteins may display more specific roles towards the substrates they target compared to their yeast counterparts.

The model organism *C. elegans*

Our lab uses *C. elegans* as the model organism because their genome has been fully sequenced and their nervous system is completely mapped. *C. elegans* neurons are not as complex as other metazoa yet retain similar neuronal organization. The position and fate of every cell in *C. elegans* has also been mapped, giving us ample information about cellular interactions. *C. elegans* are optically clear, which is important for *in vivo* imaging. About 30% of genes within *C. elegans* are highly conserved in humans, which makes them good models for studying our genes of interest in higher organisms (Kaletta and Hengartner, 2006).

The odorant receptor ODR-10

To gain more insight on ERAD's regulation of membrane proteins, we chose the Odorant Receptor-10 (ODR-10) as the protein of interest in our study. ODR-10 is a transmembrane receptor expressed specifically in the AWA neuron in *C. elegans* (Scholey, 2007). Within the amphid sensilla chemosensory organs of *C. elegans* are two amphid wing cilia neurons termed

AWA. The AWA cell bodies begin laterally in the head, and extend and terminate around the mouth in a branched formation (Bargmann, 2006). The ODR-10 protein localizes only in the membranes of the cilia of the AWA neurons in a normal animal (Sengupta et al., 1996). Due to the small number of AWA neurons and the specificity of ODR-10 expression, this sensory receptor can be studied in a small, focused region. This receptor also specifically binds to the chemoattractant, diacetyl, a byproduct of bacteria, which *C. elegans* consume (Chuang and Collins, 1968; Sengupta et al., 1996). There are no previous studies on ERAD regulation of ODR-10, therefore our study may provide new insights into neuronal ERAD mechanisms and olfactory regulation. Transgenic worms expressing ODR-10::GFP are readily available and make it a perfect candidate.

Importantly, mutations in ERAD are associated as a possible cause of neurodegeneration via ER-stress induced neuron cell death, such as in Alzheimer's and Parkinson's diseases (Zeeshan et al., 2016). Interestingly, the loss of olfactory sensation is one of the first biomarkers indicating early onset of neurodegenerative diseases (Cheng et al., 2011; Haehner et al., 2007). Little is known how olfaction declines. Misregulated olfactory receptors or the general decline in the function of neurons responsible for olfaction may both play roles. Our studies may shed light on how a basic cellular pathway could help protect neurons from processes that precede neurodegeneration and disease.

Significance

This study adds to our knowledge about ERAD regulation and its regulatory effects on transmembrane proteins within multicellular organisms. Through our study, we have also gained insight on sensory receptor regulation and behavioral effects caused by mutations in the ERAD ubiquitination pathway. There is still little known about the mechanism of E2 and E3 ligase interactions within organisms and also across organisms. Understanding how the E2 and E3 ligase proteins interact is essential to understand what substrates are maintained under different interactions within ERAD. If specific E2 or E3 proteins are no longer present we need to understand what type of proteins and which proteins may be misregulated as a result.

Our findings could help determine possible treatments and even prevention of certain degenerative symptoms. A recent study demonstrates the E3 ubiquitin ligase HRD-1 is capable of reducing ER stress and preventing apoptosis when introduced into an Alzheimer's model organism and Parkinson's model organism (Kaneko, 2012). HRD-1 is directly regulating proteins linked to be responsible for onset of neurodegeneration in Alzheimer's and Parkinson's patients (Kaneko, 2012; Zeeshan et al., 2016). Based on this finding a treatment could possibly be developed to incorporate more HRD-1 and other E3 ligases like it into neurons to reduce degeneration. It is possible other E3 ligases involved in ERAD may also be responsible for regulating proteins that induce symptoms of neurodegenerative diseases. This further underlines the importance of understanding protein degradation pathways, such as ERAD, in relation to neurodegenerative diseases.

Questions and Hypotheses

Are olfactory recptors regulated by ERAD?

Our overall question addresses whether or not olfactory receptors are regulated by an ERAD mechanism. No studies have demonstrated a direct link between olfactory regulation and ERAD. However, olfactory receptors are transmembrane proteins, which are subjected to go through the secretory pathway, and therefore through the ER, the site of ERAD. We are not going to study all olfactory receptors, but we need one representative candidate. ODR-10 works well as that candidate. The possibility of ODR-10 being subjected to ERAD regulation is high due to being present and folded at the site where ERAD regulates for misfolded proteins. We hypothesize that if ODR-10 protein maintenance is regulated at the ER then ODR-10 is subjected to ERAD regulation.

1) Is ODR-10 regulated by an ERAD mechanism that involves the known ubiquitin pathways? We set three specific aims to address our central question. Our first aim is directed at the ubiquitin pathway in ERAD. We hypothesize that if ODR-10 maintenance is affected by loss of E3 ligase proteins then there is a specific ERAD mechanism targeting misfolded ODR-10. The relationships between the E2 and E3 proteins involved in ERAD in *C. elegans* have been characterized to an extent (Sasagawa et al., 2007). However, it is still unknown if both E2 proteins, UBC-6 and UBC-7, are required to work in tandem to ubiquitinate a target substrate or if they work separately and are specific for which E3 ligase they will interact with. We have demonstrated possible interactions by mutating the E2 and E3 ligase proteins involved in ERAD and testing whether these mutations affect ODR-10 expression and/or localization. Since most

studies of ERAD do point to an ubiquitin pathway it is not surprising to find a localization effect on ODR-10, but we have found a broad variation of localization effects depending on which E2 or E3 protein is mutated.

2) Do the E3 ligases selectively target ODR-10? Misfolded sensory receptor targeting by either specific or all E3 ligases in *C. elegans* is also unknown. Our second aim addresses whether or not the E3 ligases selectively target ODR-10. We hypothesize that if we see varying effects by loss-of-function mutations in the E3 proteins on ODR-10 expression, then there is an E3 ligase that targets ODR-10 in the ubiquitin mechanism. We addressed this question by first discerning if any of the E3 ligases involved in ERAD, HRD-1, HRDL-1, or MARC-6, affect ODR-10 expression. After observing localization effects of ODR-10::GFP, we determined the extent to which each E3 ligase effects ODR-10 localization and abundance at the cilia. All E3 ligases show some type of effect on ODR-10 localization, however some more than others.

3) Is one E2 protein sufficient for proper regulation of ODR-10 or are both required? In one model based on research in yeast, each E3 ligase has a specific E2 protein with which it interacts in the ERAD pathway. An alternative yeast model suggests both UBC-6 and UBC-7 are required to create a polyubiquitin chain. Our third specific aim addresses whether a single E2 protein is sufficient for regulation of ODR-10. We identified the localization effects of each E3 ligase and in turn determined the effects of putative loss-of-function mutations in the E2 proteins. Based on my findings we determined that both putative loss-of-function E2 mutations had an effect on ODR-10::GFP localization. Mutations in UBC-6 and UBC-7 resulted in mislocalization effects and abundance at the cilia. This may suggest that both E2 proteins must be functional in order to properly regulate misfolded ODR-10 or that one specific E2 protein is interacting with a specific E3 ligase. Based on the information we gathered with the additional

E3 mutational effects we can determine a potential ERAD ubiquitination mechanism regulating ODR-10.

Are there changes in ODR-10-dependent behavior in the presence of ERAD mutations?

We observed localization defects and changes in abundance of ODR-10::GFP when mutations were introduced in both E2 and E3 proteins of ERAD. Based on qualitative and quantitative analysis, there is an increase in ODR-10::GFP ciliary fluorescence in the ERAD mutant animals in addition to the mislocalization. Therefore, our second main question addresses whether changes in ODR-10 abundance and localization in animals that harbor mutations in ERAD genes also have changes in ODR-10-dependent behavior. We hypothesize that if deficiencies in ERAD genes are causing an increase in ODR-10::GFP abundance then the behavioral phenotype of chemotaxis will be impaired. The increase in fluorescence suggests that increased levels of ODR-10 - either functional or damaged protein - is escaping the ER and making its way to the cilia. If either cause is the case, it is possible either could be impairing chemoattraction by too much functional protein or too little functional protein. We addressed this question by performing chemotaxis assays to the attraction of diacetyl, the ligand of ODR-10. Interestingly, we observed the E2 and E3 mutant animals portray varying effects in chemoattraction.

Are UBC-6 and UBC-7 localized at the ER in the AWA neuron?

In addition to addressing the ERAD ubiquitin pathway within *C. elegans*, we wanted to characterize UBC-6 and UBC-7 in *C. elegans*, specifically in the AWA neurons. It is not known if both E2 proteins are expressed in the AWA neurons, and if they are where they localize. We addressed the question: Are UBC-6 and UBC-7 localized at the ER in the AWA neuron? We hypothesize that if the E2 proteins are expressed in the AWA neuron then they are localized at the ER, and possibly within the ER membrane, as observed in yeast (Boban et al., 2014; Deng and Hochstrasser, 2006). To address this question we engineered transgenic animals containing the E2 protein coding sequence fused with GFP downstream of the *odr-10* promoter to track the localization of these proteins within the AWA neurons.

METHODS

C. elegans husbandry and strains

All *C. elegans* strains were derived from the wild type Bristol strain N2. Strains were grown at 20°C on nematode growth medium in 60mm plates. The *E. coli* strain OP-50 was used to feed the worms in all experiments. See Table 1 for a list of alleles and transgenic strains used in this study.

Qualitatively Observing ODR-10::GFP localization in E2 and E3 mutants

Engineering the E2 and E3 mutant hybrids

To determine if ODR-10 expression is affected by mutations in the E2 and E3 proteins involved in ERAD, we bred hybrids strains of E2 and E3 mutants expressing a reporter gene for ODR-10 localization. The strain with an integrated sequence of *odr-10* promoter driving ODR-10 attached to GFP (Podr-10::ODR-10::GFP) (CX3344 *kyIs53*). To introduce E2 and E3 mutants in the ODR-10::GFP background, we crossed the mutants into the CX3344 *kyIs53* strain. The Dahlberg lab also had access to the Million Mutation Project (MMP) kit. This kit contains 2,007 mutation strains of *C. elegans* and all alleles have been fully sequenced. Through this kit we identified alleles expected to confer loss of function or knock out mutations in the E2 and E3 genes of interest.

E3 Mutations. The *hrdl-1* and *hrd-1* alleles, (*gk28* and *tm1743* respectively), are considered loss of function mutations with large regions deleted near the N-terminus (Table 1 &

Figure 2). The *marc-6* strain VC20284 (*gk121407)*, is a nonsense mutation corresponding to W391stop (Table 1 & Figure 2). This premature stop is uncharacterized but a putative loss of function allele due to loss of the transmembrane domain near the C-terminus.

E2 Mutations. *ubc-6* and *ubc-7* alleles are part of the MMP kit, and all strains are single nucleotide polymorphisms that cause a missense mutation in the protein. Some of these strains have a missense mutation in the ubiquitin conjugating catalytic (UBCc) domain. This domain in the E2 protein is responsible for binding to ubiquitin proteins and interacting with E3 ligases (Baptista et al., 2012). Because it is highly conserved across taxa, a mutation in the UBCc domain or to helical bundles that may play a role in maintaining UBCc folding has a higher chance of producing a loss of function allele. The *ubc-6* strain VC20545 (*gk146975)* contains a missense mutation at T158I (Table 1 & Figure 3). This mutation from threonine to isoleucine is nonconservative and within the C-terminal helical bundle (Unpublished work, T. Ritterhoff) directly downstream of the UBCc domain (Figure 3 & 6). This nonconservative mutation could cause a conformation change blocking the site for interaction with E3 ligases. The chosen *ubc-7* strain VC40870 (*gk857464)* contains a missense mutation at P79L (Table 1 & Figure 6). This proline is highly conserved across taxa and is only 8 amino acids from the catalytic cysteine (Figure 4). The nonconservative mutation from proline to leucine may cause structural change in the protein causing the catalytic cysteine to be unable to interact with ubiquitin.

Mutant crossing. E2 and E3 mutant hermaphrodites were crossed with male CX3344 (*kyIs53)* worms. The ODR-10::GFP allele is on the X chromosome, therefore using carrier males will produce heterozygous hermaphrodites. Once offspring were produced by the E2 or E3 mutant hermaphrodite, the presence of male offspring also indicates a successful cross with the male carriers. Hermaphrodite offspring were then individually picked and transferred to new

plates. These offspring (F1 generation) are all heterozygous for the mutant allele and ODR-10::GFP. Once F2 offspring were produced by each F1 parent, the F1 parent was lysed and reconfirmed as being a carrier of ODR-10::GFP through PCR, using the LD5 forward and LD4 reverse primers which amplify the beginning of the coding sequence of ODR-10 and ends after the GFP coding sequence (Figure 2). Worm lysis is performed by combining lysis buffer and Proteinase-k (PK) (1µl 20mg/ml PK per 100µl lysis buffer). 1µl of the lysis solution is used per individual worm and undergo lysis in the thermocycler at 65°C for 45 minutes, and 95°C for 15 minutes. Worm lysis is then ready to use for PCR. The F2 offspring from carrier F1 parents were then transferred to plates, individually. Some F2 offspring were homozygous for both the mutant allele and ODR-10::GFP. Once offspring were produced by the F2 parents, the parents were lysed and the DNA region surrounding the mutant allele is amplified via PCR, using their respective primers for amplification (Table 2). *hrd-1*, *hrdl-1*, and *marc-6* mutations can be determined based on PCR products and gel electrophoresis. *hrd-1* detection requires a one-step PCR and *hrdl-1* detection requires a two-step PCR. *marc-6* detection uses a two-step PCR technique followed by a restriction digest with the restriction enzyme EarI. For *ubc-6* and *ubc-7*, the amplified sequence via PCR was sent off for sequencing (MCLABs) in order to determine if the parent was homozygous for the mutant allele by observing the substitution point mutation locations. Parents that were confirmed mutant homozygotes were screened for ODR-10::GFP homozygosity. This was done by lysing 8 individual F3 offspring per plate and then screening for ODR-10::GFP presence via PCR as described above. If all 8 offspring show a band for ODR-10::GFP, then that plate is homozygous for ODR-10::GFP. If no plates were homozygous for either allele or just one, offspring were individually picked again and then rescreened until a homozygous line was found.

Fluorescent imaging

Once mutant crosses were made with E2 and E3 mutations, we imaged the crosses to determine changes in ODR-10::GFP expression and localization in comparison to wild type and between alleles. The level and localization of fluorescent-tagged ODR-10::GFP was first analyzed qualitatively. A Leica DMi6000 fluorescent microscope, HCX PL FLUOTAR 40X/0.60 CORR PH2 objective, and Leica DFC3000 G camera were used to image the fluorescence expression patterns. The GFP fluorescence filter was used and images were taken at 400X (total magnification), exposure time at 1 second, gain at 4, and camera acquisition at 12 bit. Adult gravid animals were randomly chosen from plates that were not starved or overcrowded. Plates were usually 4 days old. Images were taken as Z stacks beginning at the top of the worm where cilia fluorescence began to focus, and ending at the bottom of the worm where cilia fluorescence began to fade again, the point where cilia fluorescence was no longer in focus. 10 images in the Z-plane were taken for each worm. Z stacks were adjusted to include all visible fluorescence present in the head of the worm, from cell body region to nose. Z stacks were combined into one image using Z Project by maximum intensity projection using ImageJ.

Quantitatively analyzing ODR-10::GFP fluorescence

For quantifying fluorescence, 20 gravid animals per strain were chosen and imaged as described above. To determine fluorescence levels over the distance of the line, the Plot Profile tool within Analyze was used. Background fluorescence was then determined by observing the

intensity levels in the non-fluorescent section of the worm; the line would typically level out at a certain intensity. The determined background intensity was then used for all values of that worm. Ciliary fluorescence was quantified by tracing individual cilia within the animal using the segmented line tool, and line width was adjusted to include all fluorescence on that particular cilium. Using the Plot Profile tool, a list of intensities over distance of the line is listed. The distance, adjusted intensity, and background intensity values were used within the Shiny program. The Shiny program then provides the value of the area under the line of intensity over distance, this value is our total fluorescence intensity for that animal. To quantify multiple branches of cilia within one animal, multiple segmented lines were concatenated. The distance of the lines were added in sequence (adding the distance of the next line with the first line's distance to make a continuous distance measurement) to include the total fluorescence of all ciliary branches within the animal. To make distance continuous the first data point, a distance of 0, in the successive lines is removed. Once fluorescence quantification was collected we used Tukey's HSD statistical analysis, run in R, to test for significant differences between strains.

Behavioral chemotaxis assay for phenotypic differences in E2 and E3 mutants

Chemotaxis assays were prepared on 100mm plastic plates filled with approximately 9ml of 2% agar with salts: $MgCl_2$, KPO_4, and $CaCl_2$. Plates were evenly divided into three sections: left, middle, and right. A start marker was placed approximately one inch from the bottom of the plate in the middle of the middle section, markers for placing 0.1% diacetyl and 95% ethanol were placed at the apex of the curve on the furthest edge opposite each other in the left and right sections. 1µl of 0.2% azide, a paralytic, is placed at the diacetyl/ethanol markers first. At the left

marker, 1µl of 0.1% diacetyl (diluted 1:1000 in 95% ethanol) was placed over the spot of azide. At the right marker, 1µl of 95% ethanol was placed over the spot of azide. Worms were prepared 4 days prior by bleaching 40-50 gravid adults on seeded 60mm plates, 2 plates per strain. Bleaching solution contained 100µl water, 400µl 5N NaOH, and 500µl bleach per 1ml of solution. Worms were then washed off the plates with M9 solution. Every 3 minutes 1ml M9 was removed from the washed worms solution and 1ml of new M9 is added. Washes were repeated for a total of four times. After worms were washed, approximately 150 worms (about 5.5µl of washed worm solution) were placed on the 100mm plate at the start marker and left for two hours. Any residual M9 placed on the 100mm plate when adding the washed worms was removed with a kimwipe. After two hours worms were counted in five distinct locations: (A) paralyzed at the diacetyl spot, (B) within the left (diacetyl) region but not paralyzed, (C) in the middle region, (D) within the right (ethanol) region but not paralyzed, (E) and paralyzed at the ethanol spot. A chemotaxis index was then calculated using the equation: (A-E) / (A+B+C+D+E). A minimum of 10 chemotaxis assays per strain was performed. Chemotaxis index scores were then analyzed through Tukey's HSD statistical analysis, in R, to compare differences between all strains and wild type.

Characterizing the E2 proteins, UBC-6 and UBC-7, in the AWA neuron

Engineering plasmids for promoter analysis of the E2 ubiquitin carrying proteins

Amplifying the E2 promoter regions. To observe E2 transcriptional activity in the AWA neuron, we created plasmids containing the *ubc-6* or *ubc-7* promoter region upstream of

GFP. We designed primers to amplify the promoter regions of *ubc-6* and *ubc-7* with restriction sites BamHI (5' end) and HindIII (3' end) included on the ends of the amplified regions (Table 3). Promoter regions were amplified via PrimeStar PCR, and then purified by a gel DNA extraction kit by ThermoFisher.

Creating the E2 promoter reporter plasmids. A preexisting plasmid containing the *odr-10* promoter upstream of GFP (pOdr-10::GFP) containing ampicillin resistance, was used as the parent plasmid for reporter construct engineering. Restriction enzyme recognition sites BamHI (5' end) and HindIII (3'end) flank the *odr-10* promoter region within the plasmid. The parent plasmid was cut at these sites using a restriction enzyme digest with BamHI and HindIII restriction enzymes at 37 degrees Celsius. The cut parent plasmid was then purified via the Thermofisher DNA gel extraction kit. The amplified E2 promoter regions, described previously, were then placed in the cut vector via ligation (Figure 6). Competent DH5α *E. coli* cells were then transformed with the newly made plasmid via heat shock transformation. Transformed cells were plated on Luria Broth plates with ampicillin and successful transformations were screened via ampicillin resistance. Surviving colonies were then picked and screened via PCR, using the E2 promoter primers, to determine the correct promoter insert was applied to the plasmid. Colonies with correct insert were then picked and DNA was isolated via a Qiagen Plasmid Mini-prep kit. Isolated DNA was then sequenced at MCLABs to determine if any mutations occurred during amplification. Successful plasmids were then used to create transgenic animals.

Engineering plasmids for *in vivo* protein localization analysis.

To determine localization patterns of UBC-6 and UBC-7 in the AWA neuron we created plasmids containing GFP fluorescent-tagged *ubc-6* and *ubc-7* coding sequences. The plasmid containing P*odr-10*::GFP was used and coding sequences of *ubc-6* and *ubc-7* were inserted downstream of the *odr-10* promoter. ODR-10 is specifically expressed in the AWA neuron and we hoped to contain UBC-6/7 fluorescent expression to this neuron by utilizing the *odr-10* promoter. We designed primers to amplify the coding sequences of the E2 genes. Two different sets of primers were designed (Table 4): 1) A primer set that will insert the open reading frames of the E2 genes upstream of GFP and downstream of the *odr-10* promoter. 2) A primer set that will allow GFP to be inserted upstream of the *ubc-7* open reading frame and directly after the start codon downstream of the Odr-10 promoter. Protein domains in UBC-6 and UBC-7 indicate the C-terminus may be important as highly conserved domains are present near this region (Marchler-Bauer et al., 2015). To account for this, plasmids were designed so that GFP could be inserted either upstream or downstream of the open reading frame. The designed primers include KpnI restriction sites on both ends on the coding sequences. A single KpnI restriction site was located downstream of the *odr-10* promoter and upstream of the GFP coding sequence in the plasmid. Amplified coding sequences were inserted into the plasmid at this location by restriction enzyme digest and ligations (Figure 7). Competent DH5α cells were transformed with the plasmids containing the coding sequence inserts. Successful transformations were screened by selective pressure to ampicillin resistance provided by the introduced plasmid. Surviving colonies were picked and screened by directional PCR to determine if the correct insert was obtained. Colonies that contained the correct insert were selected and DNA extracted via column

purification. Isolated DNA was amplified by the corresponding primers and sequenced via the company MCLABs to determine there are no underlying mutations within the sequence.

Generating transgenic worms for UBC-6 and UBC-7 GFP expression of protein localization.

The created plasmids containing either the E2 coding sequence were then injected into wild type *C. elegans*. Plasmid DNA was introduced into the germline of animals using injection courtesy of the Ailion Lab at the University of Washington and Dr. Lina Dahlberg. Transgenic animals were co-injected with the reporter construct P*ttx-3::dsRed* for screening successful uptake of the DNA. Promising lines are stored at -80° Celsius.

RESULTS

Regulation of ODR-10 by ERAD

To address whether ODR-10 is regulated by ERAD, putative loss-of-function mutations in the E3 ligases, HRD-1, HRDL-1, and MARC-6, were crossed into animals containing integrated ODR-10::GFP. Because ERAD does regulate secretory pathway substrates, the E3 ligases should be able to target any misfolded substrate regulated within the ER. Therefore, at least one E3 ligase mutation should result in a localization defect for ODR-10::GFP if ODR-10 regulated by ERAD ubiquitination. Initially, we determined that there was mislocalization consistently in the *hrdl-1* animals; we therefore we went forward with screening all three E3 ligase putative knockouts. The E2 mutants were also not available as putative knock out alleles. Therefore in the absence for a strong candidate for a null-allele in the E2 genes, it was logical to begin studies with the E3 mutants.

The HRD-1 mutation (*tm1743*) is a 473bp deletion and subsequent 38bp insertion (Figure 2). This deletion results in the removal of the second half of exon 1 and almost all of exon 2 (Figure 2). Due to such a large region of the *hrd-1* gene removed, *hrd-1* is most likely a null allele, resulting in no functional protein product. The HRDL-1 putative loss-of-function mutation (*gk28*) is a 1981bp deletion that results in the removal of 5 of the 6 exons from the *hrdl-1* coding sequence (Figure 2). This large deletion also most likely causes a loss-of-function mutation because most of the protein sequence has been removed. MARC-6 is known to target cytosolic and nucleoplasmic proteins, therefore substrates targeted by MARC-6 should differ to HRD-1 and HRDL-1 targets (Sasagawa et al., 2007). We expected if HRD-1 and HRDL-1 effected ODR-10::GFP localization, then MARC-6 may not have an effect as it may not target the same substrates as HRD-1 and HRDL-1. However, this is not always the case. Doa10, the homolog of

MARC-6, targets Ste6*, a multispanning transmembrane protein with a cytosolic mutation. But, Ste6* can also be targeted by Hrd1, the homolog of HRD-1 (Huyer et al., 2004). In yeast, the TD domain and CTE domain of Doa10 are responsible for substrate interaction and specific targeting (Zattas et al., 2016). These domains are located in exons 5-8, which are no longer present in the *marc-6 (gk121407)* mutant (Figure 2). Removal of the TD and CTE domains should result in a loss of interaction with target substrates and therefore loss of function of MARC-6.

To determine if the E3 mutant alleles crossed in the ODR-10::GFP background caused localization defects, adult worms of each genotype were randomly selected and imaged. Images were categorized into five categories of ODR-10::GFP localization: no visible expression, ciliary fluorescence, cell body localization with/without ciliary fluorescence, aggregation (bright accumulation) in the neurite with/without ciliary fluorescence, and aggregation in the neurite aggregation, cell body, and cilia expression altogether.

The strain CX3344 *kyIs53* expresses ODR-10::GFP under the *odr-10* promoter, and is considered wild type (Table 1). Based on qualitative analysis, ciliary ODR-10::GFP fluorescence is visible in only ~55% of the worms observed expressed ciliary fluorescence (Figure 8). The ciliary fluorescence we did find was also very dim (Figure 9). No wild type animals observed expressed any other type of localization other than ciliary fluorescence (Figure 8 & 9).

In contrast, all E3 ERAD mutants caused mislocalization in varying patterns of expression. In *hrdl-1* animals, there is a higher frequency of ODR-10::GFP expression in the animals compared to wild type and ~94% display any visible ODR-10::GFP expression (Figure 8). *hrdl-1* animals have the largest percentage of mislocalization among all E3 mutants. The *hrdl-1* mutation results in cell body fluorescence and also cytosolic aggregation patterns (Figure 10). Cell body expression with or without ciliary fluorescence in *hrdl-1* animals is the most

frequent among all E3 mutants: ~70% of the animals observed contained this expression pattern (Figure 8).

Aggregation of ODR-10::GFP with or without ciliary fluorescence in *hrd-1* was not observed, however a combination of neurite aggregation, cell body expression and ciliary fluorescence are observed in ~18% of the animals (Figure 8). An array of localization effects was observed of ODR-10::GFP with the *hrd-1* mutation (Figure 11). *hrd-1* mutants often frequently displayed an increase in ODR-10::GFP fluorescence in the animal: 74.3% overall expressed ODR-10::GFP, about ~20% more often than wild type animals (Figure 8). Interestingly *hrd-1* animals had increased cell body fluorescence and cytosolic aggregation within the neurites of the AWA neurons, which is not present in wild type ODR-10::GFP worms. Expression of ODR-10::GFP in cilia was the most frequently observed localization pattern with 51% of the *hrd-1* animals observed expressing only ciliary fluorescence. Cell body fluorescence with or without ciliary fluorescence was observed in 14.3% of the animals (Figure 8). The cytosolic aggregation in the neurite is only observed at the anterior end of the neurite, just posterior to the cilia. In *hrd-1* animals 5.7% expressed aggregation in the neurite with or without ciliary fluorescence and another 2.8% expressed a combination of aggregation in the neurite, cell body fluorescence, and ciliary fluorescence (Figure 8).

ODR-10::GFP animals with the *marc-6* mutation show similar mislocalization effects as the *hrdl-1* and *hrd-1* mutants (Figure 12). ODR-10::GFP fluorescence was increased compared to wild type, with similar frequency compared to both *hrdl-1* and *hrd-1* mutants. ~84% of *marc-6* animals displayed fluorescence expression (Figure 8). Interestingly, cytosolic aggregation in the neurite with or without ciliary fluorescence was observed at a much higher frequency in *marc-6* than *hrdl-1* and *hrd-1* where ~32% display this expression pattern (Figure 8). In addition,

~16% of *marc-6* animals displayed aggregation in the neurite, cell body expression, and ciliary fluorescence (Figure 8).

The most effects on ODR-10::GFP differed between *hrdl-1*, *hrd-1*, and *marc-6*. Overall, cell body expression with or without ciliary fluorescence is the most frequent with the *hrdl-1* mutation, which also displayed the highest frequency of overall visible ODR-10::GFP fluorescence (Figure 8). The greatest increase in visible cilia fluorescence alone occurs in the *hrd-1* mutation. Both HRD-1 and HRDL-1 are homologs of the Hrd1 E3 ligase in yeast (Sasagawa et al., 2007). The similar mislocalization effects on ODR-10::GFP may be due to both targeting the same or similar substrates in the ER lumen. Lastly, cytosolic aggregation at the anterior end of the neurite near the cilia is most frequent phenotype found in the *marc-6* mutants. Overall, all three E3 ligase mutants displayed varying levels of fluorescence as well, in addition to higher frequencies of visible ODR-10::GFP fluorescence in comparison to wild type. The observed mislocalization effects of ODR-10::GFP indicate ERAD regulates ODR-10, either directly or indirectly.

Mutations in the E2 proteins result in mislocalization of ODR-10::GFP

All E3 ligase mutations individually confer changes on localization and the frequency of ODR-10::GFP fluorescence. Since all E3 ligase mutations affect ODR-10::GFP localization, it is likely that ODR-10::GFP is regulated by ubiquitination within ERAD. Our next step was to determine one or both of the E2 ubiquitin carrying ligases, UBC-6 and UBC-7, regulate ODR-10. The E2 proteins interact with the E3 ligases to synthesize polyubiquitin chains on the target substrate. Based on our results with the E3 mutants, we suspect all E3 ligase proteins are able to

target ODR-10::GFP. Therefore, it is likely that both UBC-6 and UBC-7 are involved in regulating ODR-10::GFP, regardless of whether they work separately or together.

The UBC-6 mutant allele (*gk146975*) contains a point mutation at amino acid residue 158, which resides within the helical bundle within the C-terminus of the UBC-6 protein (Figure 2). This helical bundle is thought to be responsible for interaction with the E3 ligases (Pruneda et al., 2012). The mutation results in a nonconservative missense mutation from threonine to isoleucine, which potentially causes disruption of the helical bundle due to the change in polarity on the side chain; it is therefore is a putative loss of function mutation. The UBC-7 mutant allele (*gk857464*) contains a point mutation resulting in a nonconservative missense mutation at P79L (Figure 2). This mutation is only 8 amino acids away from the evolutionarily conserved catalytic cysteine, which is responsible for interaction with the activated ubiquitin proteins (Papaevgeniou and Chondrogianni, 2014). Although proline and leucine are both nonpolar, they are structurally different enough to cause a disruption in the catalytic pocket of UBC-7, and in turn change the interaction interface with the catalytic cysteine nearby. Overall, both E2 alleles are likely loss of function mutations, and will affect ODR-10::GFP localization if they play a role in misfolded ODR-10 degradation. In order to determine this we imaged E2 mutants in the same manner as E3 mutants in the ODR-10::GFP background.

Both E2 mutations cause ODR-10::GFP mislocalization. Our image analysis of *ubc-6* in the ODR-10::GFP background displays a variety of mislocalization and qualitative observation of an increase in ODR-10::GFP fluorescence intensity (Figure 13). We observe an increase in overall ODR-10::GFP expression compared to wild type. ~75% of *ubc-6* animals imaged had visible ODR-10::GFP expression (Figure 8). We also observed cell body fluorescence with or without ciliary fluorescence in ~17% of the *ubc-6* animals. ~14% of *ubc-6* animals had a high

percentage displaying aggregation in the neurite with or without ciliary fluorescence (Figure 8). In addition, ~26% of *ubc-6* worms displayed aggregation in the neurite with cell body and ciliary fluorescence (Figure 8). Strikingly, 100% of the *ubc-7* animals had visible ODR-10::GFP expression (Figure 8 & 14). This is the largest increase in visible fluorescence expression compared to wild type animals – an ~80% increase overall. Qualitative observations also indicate an increased ODR-10::GFP fluorescence intensity at the cilia (Figure 14). All *ubc-7* animals displayed cell body fluorescence and ~57% of the animals displayed aggregation in the neurite and ciliary fluorescence, in addition to the cell body expression (Figure 8).

Overall, both of the E2 mutations caused mislocalization of ODR-10::GFP. *ubc-7* mutant animals display the most extensive change in ODR-10::GFP expression compared to wild type in which all had expression and all worms contained cell body fluorescence (Figure 8 & 14). In addition to the E3 ligase mutants, all ERAD mutations have an effect on localization patterns of ODR-10::GFP. However, all ERAD mutants displayed varying effects, and no two mutant background were precisely alike. Our data shows that *hrdl-1* and *ubc-7* mutant animals have the greatest effect on ODR-10::GFP localization and overall increase in expression (Figure 8).

Mutations in ERAD quantitatively increase ODR-10::GFP present in the cilia

We observed changes in ODR-10::GFP localization in all E3 and E2 mutant animals in comparison to wild type. We also observed an increase in ODR-10::GFP fluorescence intensity at the cilia of the ERAD mutant animals. In order to determine if ODR-10::GFP abundance is significantly different between the mutant strains and wild type, we quantitatively analyzed fluorescence intensities with ImageJ. The cilia in the nose were identified based on their

fluorescence, and were traced so that overall fluorescence in the cilia could be quantified (n=20 per strain). To determine if ciliary fluorescence intensity is significantly different in comparison to wild type we used the Tukey's HSD statistical analysis. In our qualitative analysis, increased ODR-10::GFP fluorescent intensity at the cilia are more consistent in the *hrdl-1* and *ubc-7* mutants than the *hrd-1, marc-6*, and *ubc-6* animals. Therefore, we expected higher fluorescence levels in all mutants, but more so in *hrdl-1* and *ubc-7*.

The wild type ODR-10::GFP fluorescence at the cilia is dim (Figure 15). In contrast fluorescence intensity is significantly higher in two ERAD mutants. In *hrdl-1* animals, ODR-10::GFP ciliary fluorescence intensity is significantly higher than wild type ($p < 0.05$) (Figure 15). *ubc-7* animals are even brighter and have significantly higher intensity compared to wild type ($p < 0.005$) (Figure 15). The *ubc-7* animals have the highest level of ODR-10::GFP expression in the cilia among all ERAD mutants. *hrd-1*, *marc-6*, and *ubc-6* animals did not have significantly different ciliary ODR-10::GFP expression compared to wild type ($p > 0.05$) (Figure 15). The *marc-6* animals varied more in ODR-10::GFP expression in cilia. The large degree of variation of ciliary fluorescence observed is likely due to a low number of animals containing very bright aggregates of ODR-10::GFP in the cilia. These animals had their fluorescence concentrated in a short distance. The *hrd-1* and *ubc-6* animals had a fluorescence intensity range closer to that of wild type and were not significantly different compared to wild type (Figure 15).

Interestingly, the E2 and E3 mutations with the greatest fluorescence intensity also have a greater effect on mislocalization of ODR-10::GFP. This may indicate a possible pathway in which HRDL-1 and UBC-7 regulate ODR-10, either directly or indirectly. The *hrd-1*, *marc-6*, and *ubc-6* animals have no significant difference in fluorescence intensity and also show more intermediate ODR-10::GFP mislocalization. Ciliary fluorescence quantified is a readout for the

abundance of ODR-10::GFP localized at the cilia. Our data shows a positive relationship between the degree of mislocalization of ODR-10::GFP and ciliary fluorescence intensity. These results indicate the greater number of animals mislocalizing ODR-10::GFP correlates with greater abundance of ODR-10::GFP in the cilia.

Chemoattraction is impaired with the loss of ERAD ubiquitin proteins

The increased fluorescence and mislocalization of ODR-10::GFP in our E2 and E3 mutant animals might confer a change in behavioral phenotypes such as chemoattraction to diacetyl, the ligand of ODR-10. This could be due to misfolded or damaged ODR-10::GFP being improperly trafficked from the ER to the cilia. We expect to see impairment in chemotaxis if this is the case. Another possibility would be an increase in functional ODR-10::GFP localizing in the cilia due to increased transcriptional and translational activity. An increase in functional ODR-10 could also overwhelm the neuron and have underlying effects on chemotaxis beyond a normal worm. In order to assess the consequences of increased ODR-10::GFP abundance at the cilia, we measured the efficiency of chemoattraction in wild-type animals, and those harboring mutations in ERAD genes. Chemoattraction assays were performed for all mutants with diacetyl on one side of a 100mm plate and ethanol, which *C. elegans* is not attracted to, on the other side. Animals that made it to either region remain there due to paralysis caused by azide. Assays were quantified based on a chemotaxis index with a range of -1 (all animals at ethanol) to +1 (all animals at diacetyl). To determine if there was statistical significance between wild type animals and ERAD mutants, we determined p values by Tukey's HSD analysis.

Wild type (N2) animals have a high chemotaxis index, with ~80% of animals moving to the diacetyl (Figure 16). Animals containing a non-functional allele of the *odr-10* gene were used in order to determine what a chemotaxis index should be if ODR-10 was completely absent (the negative control) (Ryan et al., 2014). *odr-10* animals have a chemotaxis index close to 0 indicating no preference to move towards diacetyl or ethanol (Figure 16). In contrast the ERAD mutants all have chemotaxis indices between wild type and *odr-10,* and all are significantly different compared to wild type and *odr-10* ($p < 0.05$). *hrd-1* animals have the highest chemotaxis index compared to all the ERAD mutants (Figure 16). The *marc-6 and ubc-6* animals have chemotaxis indices just below *hrd-1* animals (Figure 16). *hrd-1*, *marc-6,* and *ubc-6* animals all have intermediate chemotaxis impairment compared both to wild type and *odr-10*. The intermediate chemotaxis impairment suggests a trend that reflects the more intermediate effects that these ERAD mutants confer on localization and abundance of ODR-10::GFP. In contrast, *hrdl-1* and *ubc-7* animals have the lowest chemotaxis indices suggesting a greater impairment in chemoattraction similar to *odr-10* knock out animals. Our results suggest a relationship of higher chemotaxis impairment with greater mislocalization of ODR-10::GFP (Figure 16).

The E2 mutant animals also show similar chemotaxis impairment to the E3 ligase mutants. The *ubc-7* putative knockdown animals had a much lower chemotaxis index in comparison to the *ubc-6* animals. The *ubc-7* animals have a chemotaxis index similar to that of *hrdl-1* and *odr-10* animals, and had the lowest chemotaxis index of all the ERAD mutants (Figure 16). The *ubc-6* animals have a chemotaxis index that was more intermediate, similar to *hrd-1* and *marc-6* animals (Figure 16). Through Tukey's HSD analysis, both E2 mutants have significantly lower chemotaxis indices than wild type animals ($p < 0.005$) and are also significantly higher than *odr-10* knock out animals.

Altogether, our data shows a relationship in which the animals with mutations that confer greater ciliary fluorescence intensities also display the most impaired chemotaxis. *hrdl-1* and *ubc-7* animals have the greatest effect on overall presence of ODR-10::GFP fluorescence, mislocalization of ODR-10::GFP, highest ciliary fluorescence intensities, and the lowest chemotaxis indices of the ERAD mutants. *Hrd-1*, *marc-6*, and *ubc-6* do display effects on ODR-10::GFP localization and chemotaxis, however all three have a more intermediate trend and are less severe than *hrdl-1* and *ubc-7* animals.

E2 ubiquitin proteins localize at the ER in *C. elegans*

We predict that the E2 ubiquitin proteins are universally involved in ERAD in all cells within *C. elegans*, however this has yet to be shown. Based on the mechanism that the E2 proteins either work together or individually with different E3 ligase proteins this is likely true. The localization of the E2 proteins is also not known in *C. elegans*. It is likely that both proteins localize to the ER, the site of ERAD. This is supported by the fact that both E2 proteins contain ER membrane association domains (Boban et al., 2014; Deng and Hochstrasser, 2006). Based on the localization defects of ODR-10::GFP and chemotaxis impairment in the absence of wild type *ubc-6* and *ubc-7,* it is likely both E2 proteins are present in the AWA neuron. We wanted to determine the localization of the E2 proteins and designed transgenic animals that include coding sequences of both E2 proteins downstream of the *odr-10* promoter and GFP attached on the C-terminus. The *odr-10* promoter is only active in the AWA neuron; therefore our E2 proteins with GFP should only be expressed in the AWA neurons. We observed UBC-6::GFP and UBC-7::GFP fluorescence in the cell bodies of the AWA neurons. Expression was only observed at the

cell body and we also observed expression in various stages of development. The site of ERAD, the ER, is also in the cell body (Unpublished Data, Sam Witus & Ailion Lab), which suggests that the E2 proteins are likely at the ER.

Interestingly, E2::GFP expression driven by the *odr-10* promoter was not observed in well-fed and/or uncrowded transgenic carriers. Gravid adult worms on overcrowded and starved plates were the only animals we could observe fluorescence expression, but only in about 1 in 30 worms (Data not shown). We also observed a similar increase in *odr-10* promoter activity in CX3344 (*kyIs53)* animals that were starved and overcrowded where ODR-10::GFP at the cilia was visibly brighter and cell body expression was present (Unpublished Data, Ellen Zocher). Plates are overcrowded when the number of worms on the plate exceeds the available nutrient availability and available space. Starved animals had diminished all food sources on the plate they are contained and therefore had no food available for at least 24 hours prior to imaging. When E2::GFP fluorescence was observed it was always at the cell body in the AWA neuron (Figure 17 & 18). This also supports the effects we observe our E2 mutants have on ODR-10. We can now visualize that the E2 proteins localize at or near the site of ERAD (Figure 17 & 18). Our mutations and their corresponding effects are most likely due to UBC-6 and UBC-7 playing a role in ERAD, and potentially as direct regulators of ODR-10.

DISCUSSION

The odorant receptor ODR-10 in *C. elegans* has not been studied before regarding its regulation by ERAD. Thus ODR-10 is a novel tool for studying this regulatory mechanism. The mutations of the ERAD-associated E3 and E2 proteins all have an effect on ODR-10 localization and chemotaxis, however some more than others. Our findings suggest that damaged or misfolded ODR-10 protein is normally degraded by an ERAD mechanism, and that there is specificity among the E3 ligases and cooperation between the E2 proteins for proper ODR-10 maintenance.

Results of mutations of E3 ligases

Our findings suggest that all E3 ligases can target ODR-10, however some E3 ligases potentially have a higher propensity than others to target ODR-10. Based on mislocalization patterns and fluorescence quantification, the *hrd-1* and *marc-6* mutations had a less severe effect than the *hrdl-1* mutation. Therefore, if ODR-10 is a direct target, it is most likely that HRDL-1 is the primary E3 ligase to target the ODR-10 substrate, although HRD-1 and MARC-6 can also target ODR-10 with less affinity. The *hrdl-1* mutants also more often have cell body fluorescence and have significantly increased ciliary fluorescence of ODR-10::GFP. The *marc-6* and *hrd-1* animals had lower fluorescent levels that were not significantly different than our wild type strain, CX3344 (*kyis53*). Our imaging data is supported by our chemotaxis assays in which *hrdl-1* animals were the most impaired with *hrd-1* and *marc-6* animals at a more intermediate chemotaxis index between wild type and *odr-10* knockout animals, (discussed in depth below).

Overall, when HRDL-1 is missing there is a larger effect on ODR-10 regulation and cellular upkeep, which suggests this E3 ligase has the greatest affinity to target ODR-10.

Without biochemically showing a direct relationship between ODR-10 and the E3 ligases we are unable to tell if HRDL-1 is specifically and directly targeting ODR-10 or if there is an intermediate interaction at play. One possible mechanism that could cause the phenotypes we observed is that HRDL-1 may target a different protein, which in turn affects ODR-10 regulation and chemotaxis function. There are proteins that assist in trafficking of GPCR proteins, such as ODR-10, at the ER and also at the plasma membrane (Magalhaes et al., 2012). If these proteins were to be misregulated due to the ERAD mutations we may observe similar results of ODR-10 misregulation. We also do not know if what we are observing is cell autonomous as the E3 mutations are not specific for the AWA neurons and are present in every cell in the animal. For example, the AWA neuron forms gap junctions with the AIA interneuron (Larsch et al., 2015). If the ERAD mutations cause protein misregulation in the AIA interneuron, signaling to the AWA neuron may change and then impact AWA cell activity. Therefore, the phenotypes could be due to signaling from other cells in response to the E3 mutations.

Results of mutations of E2 proteins

Based on our findings with the E2 mutant animals, both UBC-6 and UBC-7 play roles in regulating ODR-10. Mutation of either E2 protein resulted in changed in ODR-10 localization patterns, abundance, and chemotaxis impairment. The *ubc-6* mutant had a lower fluorescence intensity overall in comparison to the *ubc-7* mutant animals. Once again this may not be a direct relationship with ODR-10, but our observations that HRDL-1 may also be the primary E3 ligase

to target ODR-10 could suggest a potential mechanism of which E2 and E3 proteins are involved in misfolded ODR-10 regulation. Previous studies suggested HRDL-1 specifically interacted with UBC-6 in order to ubiquitinate substrate targets (Hirsch et al., 2009). However, a recent yeast study presents a mechanism in which both UBC-6 and UBC-7 work in tandem with their cognate E3 ligase in order to polyubiquitinate the target (Weber et al., 2016). In our animals, if HRDL-1 interacts with UBC-6, and not UBC-7, we would expect to see a more severe effect in *ubc-6* mutant animals than *ubc-7*. However, in our findings we observed a higher mislocalization effect, fluorescence intensity, and impaired chemotaxis in the *ubc-7* mutant in comparison to *ubc-6*. We also observe less severe effects in *hrd-1* and *marc-6* mutant animals and both E3 ligases are known to interact specifically with UBC-7 (Cohen et al., 2015). If HRD-1 and MARC-6 were to be the only E3 ligases to interact with UBC-7, we would expect to see similar levels of misregulation of ODR-10. However, in our study we only see intermediate effects with these E3 ligase mutants. Therefore it is unlikely that the E3 ligases interact specifically with only one E2 protein and that the E2 proteins work through entirely separate pathways.

Based on our findings, the effects we observed suggest the E2 proteins could work in tandem in order to effectively polyubiquitinate target substrates (Figure 19). The *ubc-6* mutant may have a lesser effect on misregulation of ODR-10 because if UBC-6 is absent, UBC-7 can prime and polyubiquitinate the target as well (Weber et al., 2016). Therefore, the *ubc-6* mutant animals show some effect, though UBC-7 may be able to compensate the role of UBC-6 in this context. If UBC-7 is no longer functional, however, UBC-6 is able to prime the substrate target but unable to polyubiquitinate, therefore less misfolded ODR-10 is likely degraded in *ubc-7* mutant animals (Weber et al., 2016). If this mechanism were to play a role in regulation of ODR-

10 there would be more misregulation in the absence of UBC-7. Our observations of larger effects in the *ubc-7* mutant animals support this potential mechanism.

Impaired chemotaxis

Because of the varying ODR-10::GFP localization and an increase in fluorescence presence and intensity in the ERAD E2 and E3 mutants, we expected a change in the behavioral phenotype of chemoattraction. The mislocalization and increased fluorescence of ODR-10::GFP suggests there is more of the protein present in the mutant animals. However, it is unknown if the ODR-10::GFP proteins present in these mutants is functional or misfolded. It has been shown ERAD substrates that are misfolded are able to exit the ER if they still present the correct protein structural fold for an exit signal (Kincaid and Cooper, 2007). Therefore, it is possible misfolded ODR-10 is exported to the Golgi from the ER if this exit signal is still present in their structure. This would also explain why we observe cell body fluorescence; these misfolded proteins may not present the correct exit signal in their folded structure to be exported from the ER and cause protein aggregation.

The mislocalization effects we see may be due to too much functional ODR-10 protein present and that not all of the protein can localize to the cilia. Increasing transcriptional activity for certain proteins has been shown under stress responses such as starvation and even in nonfunctional ERAD models (Larance et al., 2015; Sakaki and Kaufman, 2013). Improper or reduced ERAD ubiquitination may cause cellular stress, possibly due to other protein aggregates we have not observed in our model. These could initiate similar stress responses under ER quality control. Production of ODR-10 protein may be increased as well in response to the

absence of one of the E2 or E3 proteins involved in ERAD. This may be a stress response that increases transcription and translation of ODR-10, therefore completely functional ODR-10 is being processed and localizing to the cilia.

The increase in ODR-10 at the cilia, whether it is damaged or functional, could cause a behavioral phenotype change. If misfolded ODR-10 is localizing at the cilia, then we would expect this ODR-10 would not function and could cause impaired chemoattraction to diacetyl. If the ODR-10 is still functional but is increasing at the cilia, the overproduction of ODR-10 could be overwhelming the chemosensory neuron and we may still observe chemoattraction impairment. When exposed to diacetyl over a prolonged period of time the animals become desensitized (Larsch et al., 2015). The increased ODR-10 expression observed in ERAD mutants could be overstimulating the AWA neuron and desensitizing the animal faster than normal. This is a possibility if it is functional ODR-10 we observe in greater abundance at the cilia.

Regardless of the mechanism, we observe significant impairment in all E2 and E3 mutant animals in comparison to wild type animals. We also observe varying degrees of impairment between E3 ligase and E2 mutants. The *hrdl-1* mutant animals have the lowest chemotaxis index among the E3 ligase mutants, and these animals' chemotaxis indices were closer to the *odr-10* knockout mutant animals, though still significantly different. The *marc-6* and *hrd-1* mutant animals have a more intermediate chemotaxis index but are both still significantly less than wild type animals. Based on observations among the *hrd-1* animals, the chemotaxis assays portrayed the worms going in the direction of diacetyl, just taking much longer than the 2-hour timespan to make it to the diacetyl point. The *hrd-1* worms seemed to collect and remain at the starting point of the assay (i.e. in the middle of the assay plate) for a much longer period before moving towards diacetyl, and not many animals went in the direction of ethanol. If left for a longer

period, it is likely these animals could show similar chemotaxis indices to that of wild type. The *hrdl-1* animals were more spread out on the plates and we did not observe this trend to go solely towards the diacetyl.

The E2 mutant animals also had varying impaired chemotaxis indices and both were significantly impaired in comparison to wild type animals. The *ubc-7* mutants had a lower chemotaxis index similar to that of the *hrdl-1* animals. The *ubc-6* mutants had a higher chemotaxis index similar to the *hrd-1* and *marc-6* mutant strains. Interestingly, the *ubc-6* animals were observed to have a similar trend to be going to the direction of diacetyl similar to that of the *hrd-1* animals after 2 hours. The *ubc-7* mutants, however, were more spread out across the plate and did not show this trend. Instead, they behaved similarly to the *hrdl-1* and *marc-6* animals. Overall, the *hrdl-1* and *ubc-7* mutant animals had the lowest chemotaxis index further supporting the proposed mechanism of HRDL-1 specificity and E2 cooperation.

E2::GFP localization

Our transgenic strains for observing E2 localization enabled us to visualize the proteins localized within the cell bodies of the AWA neurons. We suspect the E2 proteins are localized at the ER membrane, the site of ERAD. Future studies should fluorescently mark the ER in these neurons and determine if the E2::GFP fluorescence we observed within the cell bodies co-localizes with the ER. We also observed nuclear localization suggesting a possible nuclear role for those E2 proteins. The expression pattern and/or cell specific expression of the E2 genes still not known, and is uncharacterized for the AWA neurons. A future study will allow us to determine the promoter activity of the E2 genes in *C. elegans*. We have designed primers and

have successfully amplified the E2 promoters, which can now be used to create plasmids with the E2 promoter region upstream of GFP. The importance of ERAD in regulating protein production and the highly involved roles both E2 proteins play suggests the E2 promoters are most likely active in every cell and therefore we expect to see promoter activity in the AWA neurons. Novel promoter reporter strains will help to demonstrate this.

E2::GFP expression was not observed very often in the P*odr-10*::*ubc-X*::GFP transgenic animals. We also only observed E2::GFP expression in starved and overcrowded animals. In well fed, uncrowded wild type (*kyIs53*) animals, we do observe increased fluorescence of ODR-10::GFP when worms undergo stressful conditions like starvation and overcrowding (Unpublished Data, Ellen Zocher). *kyIs53* contains ODR-10::GFP driven by the *odr-10* promoter, and our transgenic strains contain E2::GFP driven by the same promoter. In the P*odr.10*::*ubc-X*::GFP transgenic animals under well fed, uncrowded conditions, we did not observe E2::GFP expression. This is likely due to their expression being driven by the weak/low activity *odr-10* promoter. It is possible that the increase in expression of E2::GFP is due to the *odr-10* promoter being more active under starved and overcrowded conditions.

Another possibility could be that only a small amount of UBC-6 and UBC-7 is expressed and maintained in the cell. The UBC-6 and UBC-7 orthologs in yeast have a high turn over rate to maintain specific levels, and could also be true in *C. elegans* (Kreft and Hochstrasser, 2011; Ravid and Hochstrasser, 2007). A high turnover rate may also explain why we did not observe E2::GFP expression in normal animals as these proteins are possibly maintained at very low levels of expression.

Conclusion

In our study, we point to possible mechanisms of ERAD within *C. elegans* that could regulate the ODR-10 receptor, and therefore neural receptor proteins in general. Our findings suggest a mechanism where three E3 ligases (HRD-1, HRDL-1, and MARC-6) have some specificity for a target substrate (ODR-10::GFP), and some E3 ligases are redundant or substitute for other E3 ligases under mutant conditions. Our findings also suggest the E2 proteins, UBC-6 and UBC-7, both play roles in regulating ODR-10::GFP, and may work in tandem to degrade the misfolded protein. Indeed a recent study in yeast shows both E2 proteins work together to polyubiquitinate substrates (Weber et al., 2016). In the absence of individual ERAD functional proteins we also observe a behavioral change in the animals, which may present a case as to why certain neurological symptoms may appear in degenerative diseases.

Our data suggests a relationship between the level of impaired chemotaxis impairment and the level of ODR-10::GFP abundance at the AWA cilia. We observe these with all the ERAD mutants, with the highest extremes in the absence of HRDL-1 or UBC-7. Overall, we propose HRDL-1 is the main E3 ligase to target ODR-10 based on the relationship this E3 mutation causes the most chemotaxis impairment and highest fluorescence increase. The loss of MARC-6 or HRD-1 only shows intermediate effects, which suggests they play a lesser role in regulating ODR-10. The E2 proteins may work in tandem to polyubiquitinate ODR-10 once it is recognized by HRDL-1.

Broader Significance

Previous studies have shown that HRD-1 and MARC-6 are necessary for *C. elegans* development in the presence of long term ER stress, however HRDL-1 is not (Sasagawa et al., 2007). Here, we observe HRDL-1 is necessary for proper ODR-10 upkeep in adult animals, whereas HRD-1 and MARC-6 have a more intermediate effect. Therefore our study points to a possible role of HRDL-1 post development related to cellular upkeep in neurons that does not require HRD-1 and MARC-6.

Our study suggests that if mutations in ERAD were to exist in an organism, receptors targeted by the E2 or E3 protein could accumulation and potential aggregation at the ER in neurons. It is also possible misfolded receptors may accumulate and potentially aggregate at the ER in neurons. It is also possible misfolded receptors may accumulate at the synapse membrane and result in impairment of the phenotype the receptor is responsible for. This could be the case in humans, as there are well-conserved homologs of all three E3 ligases in *C. elegans*. The human homologs of HRD-1, HRDL-1, and MARC-6 are Hrd1, gp78, and MARCH6 respectively (Sasagawa et al., 2007). There are 6 known ERAD E3 ligases in humans, which may indicate there are more interactions and specific roles the E3 ligases may take part in in comparison to yeast and *C. elegans* (Tamura et al., 2010). Three identified E2 proteins involved in ERAD in humans, are also orthologs to the *C. elegans* E2 proteins: UBE2J1 and UBE2J2 are orthologs of UBC-6, and UBE2G2 is the ortholog of UBC-7 (Burr et al., 2011). The E2 and E3 ligase homologs interact in a similar fashion as *C. elegans,* which could suggest similar roles are played. The human Hrd1 protein interacts with UBE2J1 and gp78 interacts with UBE2G2 (Burr et al., 2011; Christianson et al., 2011). The gp78 protein also works downstream of Hrd1 in

marking substrates for degradation (Zhang et al., 2015). It is unknown which E2 proteins the mammalian MARCH6 interacts with.

Mammalian E2:E3 interactions require further study. However early investigations show some insight as to how conserved functions are across species. Interestingly, gp78 and UBE2G2 interact and our study points to HRDL-1 and UBC-7 interaction and possibly also UBC-7 and UBC-6 working in tandem. Their roles may be conserved and it would also be interesting to study if the mammalian UBE2G2 works in tandem with UBE2J1 or UBE2J2. This may be possible due to gp78's acting downstream of Hrd1 to polyubiquitinate substrates. Since gp78 interacts with UBE2G2 and Hrd1 interacts with UBE2J1, this polyubiquitination could be due to the E2 proteins working in tandem but still interacting with their respective E3 ligases. Overall, our study indicates a possibility to conserved interactions between E2 and E3 ligases involved in ERAD.

In humans, ERAD mutations may result in the loss of olfaction and possibly other impaired senses early on in neurodegenerative patients if neuronal upkeep has similar maintenance regarding HRDL-1. Identifying probable causes of mutations in ERAD ubiquitination proteins in human neurodegenerative patients could lead to a better understanding of what may be creating early symptoms. It is possible we could also develop treatments to prevent or prolong the time to onset of these symptoms if we can repair or enhance ERAD in these patients. For example, a recent study showed prolonged ER stress increased reactive oxygen species which play a significant role in neurodegenerative diseases (Zeeshan et al., 2016). In another case, Hrd1 is shown to promote the degradation of the amyloid precursor protein (APP), which is responsible for the accumulation of amyloid β protein in Alzheimer's patients. When Hrd1 is no longer present, as observed in Alzheimer's patients, there is an

increase in APP (Kaneko et al., 2012). This further suggests ERAD proteins play a role in cell maintenance and if no longer present can induce the onset of neurodegenerative symptoms.

Future Directions

To further support and clarify our findings the Dahlberg lab plans to further explore the role of the E3 ligase and E2 proteins in response to regulation of ODR-10 and also the glutamate receptor GLR-1. GLR-1 will be studied to determine if we observe a similar effect in misregulation on a different receptor expressed in different neurons. The Dahlberg lab also plans to biochemically analyze the increase in ODR-10::GFP abundance and also ubiquitin modification levels of ODR-10 in all ERAD mutant animals. We plan to determine if this increase in ODR-10 can be biochemically quantified and also determine if there is an increase in misfolded or normal receptor. These plans will further our understanding as to what may be causing the mislocalization, fluorescence increase, and chemotaxis impairment we observed of ODR-10 in ERAD mutant animals.

WORKS CITED

Araki, K., and Nagata, K. (2011). Protein Folding and Quality Control in the ER. Cold Spring Harb. Perspect. Biol. *3*, a007526–a007526.

Baptista, M.S., Duarte, C.B., and Maciel, P. (2012). Role of the ubiquitin–proteasome system in nervous system function and disease: using C. elegans as a dissecting tool. Cell. Mol. Life Sci. *69*, 2691–2715.

Bargmann, C. (2006). Chemosensation in C. elegans. WormBook.

Boban, M., Pantazopoulou, M., Schick, A., Ljungdahl, P.O., and Foisner, R. (2014). A nuclear ubiquitin-proteasome pathway targets the inner nuclear membrane protein Asi2 for degradation. J. Cell Sci. *127*, 3603–3613.

Burr, M.L., Cano, F., Svobodova, S., Boyle, L.H., Boname, J.M., and Lehner, P.J. (2011). HRD1 and UBE2J1 target misfolded MHC class I heavy chains for endoplasmic reticulum-associated degradation. Proc. Natl. Acad. Sci. *108*, 2034–2039.

Cao, S.S., and Kaufman, R.J. (2012). Unfolded protein response. Curr. Biol. *22*, R622–R626.

Cheng, N., Cai, H., and Belluscio, L. (2011). In Vivo Olfactory Model of APP-Induced Neurodegeneration Reveals a Reversible Cell-Autonomous Function. J. Neurosci. *31*, 13699–13704.

Christianson, J.C., Olzmann, J.A., Shaler, T.A., Sowa, M.E., Bennett, E.J., Richter, C.M., Tyler, R.E., Greenblatt, E.J., Wade Harper, J., and Kopito, R.R. (2011). Defining human ERAD networks through an integrative mapping strategy. Nat. Cell Biol. *14*, 93–105.

Chuang, L.F., and Collins, E.B. (1968). Biosynthesis of diacetyl in bacteria and yeast. J. Bacteriol. *95*, 2083–2089.

Chung, K.K., Dawson, V.L., and Dawson, T.M. (2001). The role of the ubiquitin-proteasomal pathway in Parkinson's disease and other neurodegenerative disorders. Trends Neurosci. *24*, 7–14.

Ciechanover, A., and Masucci, M. (2002). Ubiquitin-Proteasome Proteolytic System: From Classical Biochemistry to Human Diseases (World Scientific).

Cohen, I., Wiener, R., Reiss, Y., and Ravid, T. (2015). Distinct activation of an E2 ubiquitin-conjugating enzyme by its cognate E3 ligases. Proc. Natl. Acad. Sci. *112*, E625–E632.

Cooper, G. (2000). The Endoplasmic Reticulum - The Cell - NCBI Bookshelf.

Deng, M., and Hochstrasser, M. (2006). Spatially regulated ubiquitin ligation by an ER/nuclear membrane ligase. Nature *443*, 827–831.

Fewell, S.W., Travers, K.J., Weissman, J.S., and Brodsky, J.L. (2001). The Action of Molecular Chaperones in the Early Secretory Pathway. Annu. Rev. Genet. *35*, 149.

Habeck, G., Ebner, F.A., Shimada-Kreft, H., and Kreft, S.G. (2015). The yeast ERAD-C ubiquitin ligase Doa10 recognizes an intramembrane degron. J. Cell Biol. *209*, 261–273.

Haehner, A., Hummel, T., Hummel, C., Sommer, U., Junghanns, S., and Reichmann, H. (2007). Olfactory loss may be a first sign of idiopathic Parkinson's disease. Mov. Disord. *22*, 839–842.

Harding, H.P., Novoa, I., Zhang, Y., Zeng, H., Wek, R., Schapira, M., and Ron, D. (2000). Regulated translation initiation controls stress-induced gene expression in mammalian cells. Mol. Cell *6*, 1099–1108.

Hirsch, C., Gauss, R., Horn, S.C., Neuber, O., and Sommer, T. (2009). The ubiquitylation machinery of the endoplasmic reticulum. Nature *458*, 453–460.

Hollien, J., and Weissman, J.S. (2006). Decay of Endoplasmic Reticulum-Localized mRNAs During the Unfolded Protein Response. Science *313*, 104–107.

Huyer, G., Piluek, W.F., Fansler, Z., Kreft, S.G., Hochstrasser, M., Brodsky, J.L., and Michaelis, S. (2004). Distinct Machinery Is Required in Saccharomyces cerevisiae for the Endoplasmic Reticulum-associated Degradation of a Multispanning Membrane Protein and a Soluble Luminal Protein. J. Biol. Chem. *279*, 38369–38378.

Kaletta, T., and Hengartner, M.O. (2006). Finding function in novel targets: C. elegans as a model organism. Nat. Rev. Drug Discov. *5*, 387–399.

Kaneko, M. (2012). Molecular pharmacological studies on the protection mechanism against endoplasmic reticulum stress-induced neurodegenerative disease. Yakugaku Zasshi *132*, 1437–1442.

Kaneko, M., Okuma, Y., and Nomura, Y. (2012). Molecular Approaches to the Treatment, Prophylaxis, and Diagnosis of Alzheimer's Disease: Possible Involvement of HRD1, a Novel Molecule Related to Endoplasmic Reticulum Stress, in Alzheimer's Disease. J. Pharmacol. Sci. *118*, 325–330.

Kincaid, M.M., and Cooper, A.A. (2007). Misfolded proteins traffic from the endoplasmic reticulum (ER) due to ER export signals. Mol. Biol. Cell *18*, 455–463.

Kreft, S.G., and Hochstrasser, M. (2011). An Unusual Transmembrane Helix in the Endoplasmic Reticulum Ubiquitin Ligase Doa10 Modulates Degradation of Its Cognate E2 Enzyme. J. Biol. Chem. *286*, 20163–20174.

Larance, M., Pourkarimi, E., Wang, B., Brenes Murillo, A., Kent, R., Lamond, A.I., and Gartner, A. (2015). Global Proteomics Analysis of the Response to Starvation in *C. elegans*. Mol. Cell. Proteomics *14*, 1989–2001.

Larsch, J., Flavell, S.W., Liu, Q., Gordus, A., Albrecht, D.R., and Bargmann, C.I. (2015). A circuit for gradient climbing in C. elegans chemotaxis. Cell Rep. *12*, 1748–1760.

Lee, W., Yoo, W., and Chae, H. (2015). ER Stress and Autophagy. Curr. Mol. Med. *15*, 735–745.

Magalhaes, A.C., Dunn, H., and Ferguson, S.S. (2012). Regulation of GPCR activity, trafficking and localization by GPCR-interacting proteins: Regulation of G-protein-coupled receptor activity. Br. J. Pharmacol. *165*, 1717–1736.

Marchler-Bauer, A., Derbyshire, M.K., Gonzales, N.R., Lu, S., Chitsaz, F., Geer, L.Y., Geer, R.C., He, J., Gwadz, M., Hurwitz, D.I., et al. (2015). CDD: NCBI's conserved domain database. Nucleic Acids Res. *43*, D222–D226.

Mittal, S., Chowhan, R.K., and Singh, L.R. (2015). Macromolecular crowding: Macromolecules friend or foe. Biochim. Biophys. Acta BBA - Gen. Subj. *1850*, 1822–1831.

Moore, K.A., and Hollien, J. (2012). The Unfolded Protein Response in Secretory Cell Function. Annu. Rev. Genet. *46*, 165–183.

Olzmann, J.A., Kopito, R.R., and Christianson, J.C. (2013). The Mammalian Endoplasmic Reticulum-Associated Degradation System. Cold Spring Harb. Perspect. Biol. *5*, a013185.

Papaevgeniou, N., and Chondrogianni, N. (2014). The ubiquitin proteasome system in Caenorhabditis elegans and its regulation. Redox Biol. *2*, 333–347.

Pruneda, J.N., Littlefield, P.J., Soss, S.E., Nordquist, K.A., Chazin, W.J., Brzovic, P.S., and Klevit, R.E. (2012). Structure of an E3:E2~Ub Complex Reveals an Allosteric Mechanism Shared among RING/U-box Ligases. Mol. Cell *47*, 933–942.

Ravid, T., and Hochstrasser, M. (2007). Autoregulation of an E2 enzyme by ubiquitin-chain assembly on its catalytic residue. Nat. Cell Biol. *9*, 422–427.

Rutledge, A.C., Qiu, W., Zhang, R., Kohen-Avramoglu, R., Nemat-Gorgani, N., and Adeli, K. (2009). Mechanisms Targeting Apolipoprotein B100 to Proteasomal Degradation: Evidence That Degradation Is Initiated by BiP Binding at the N Terminus and the Formation of a p97 Complex at the C Terminus. Arterioscler. Thromb. Vasc. Biol. *29*, 579–585.

Ryan, D.A., Miller, R.M., Lee, K., Neal, S.J., Fagan, K.A., Sengupta, P., and Portman, D.S. (2014). Sex, Age, and Hunger Regulate Behavioral Prioritization through Dynamic Modulation of Chemoreceptor Expression. Curr. Biol. *24*, 2509–2517.

Sakaki, K., and Kaufman, R.J. (2013). Interaction between quality control systems for ER protein folding and RNA biogenesis. Worm *2*, e23005.

Sasagawa, Y., Yamanaka, K., and Ogura, T. (2007). ER E3 ubiquitin ligase HRD-1 and its specific partner chaperone BiP play important roles in ERAD and developmental growth in Caenorhabditis elegans. Genes Cells Devoted Mol. Cell. Mech. *12*, 1063–1073.

Scholey, J. (2007). The sensory cilia of Caenorhabditis elegans_Revised. WormBook.

Sengupta, P., Chou, J.H., and Bargmann, C.I. (1996). odr-10 Encodes a Seven Transmembrane Domain Olfactory Receptor Required for Responses to the Odorant Diacetyl. Cell *84*, 899–909.

Shen, X., Zhang, K., and Kaufman, R.J. (2004). The unfolded protein response—a stress signaling pathway of the endoplasmic reticulum. J. Chem. Neuroanat. *28*, 79–92.

Shiber, A., Breuer, W., Brandeis, M., and Ravid, T. (2013). Ubiquitin conjugation triggers misfolded protein sequestration into quality control foci when Hsp70 chaperone levels are limiting. Mol. Biol. Cell *24*, 2076–2087.

Tamura, T., Sunryd, J.C., and Hebert, D.N. (2010). Sorting things out through endoplasmic reticulum quality control. Mol. Membr. Biol. *27*, 412–427.

Travers, K.J., Patil, C.K., Wodicka, L., Lockhart, D.J., Weissman, J.S., and Walter, P. (2000). Functional and genomic analyses reveal an essential coordination between the unfolded protein response and ER-associated degradation. Cell *101*, 249–258.

Vembar, S.S., and Brodsky, J.L. (2008). One step at a time: endoplasmic reticulum-associated degradation. Nat. Rev. Mol. Cell Biol. *9*, 944–957.

Weber, A., Cohen, I., Popp, O., Dittmar, G., Reiss, Y., Sommer, T., Ravid, T., and Jarosch, E. (2016). Sequential Poly-ubiquitylation by Specialized Conjugating Enzymes Expands the Versatility of a Quality Control Ubiquitin Ligase. Mol. Cell *63*, 827–839.

Ye, Y., Shibata, Y., Kikkert, M., van Voorden, S., Wiertz, E., and Rapoport, T.A. (2005). Recruitment of the p97 ATPase and ubiquitin ligases to the site of retrotranslocation at the endoplasmic reticulum membrane. Proc. Natl. Acad. Sci. U. S. A. *102*, 14132–14138.

Zattas, D., Berk, J.M., Kreft, S.G., and Hochstrasser, M. (2016). A Conserved C-terminal Element in the Yeast Doa10 and Human MARCH6 Ubiquitin Ligases Required for Selective Substrate Degradation. J. Biol. Chem. *291*, 12105–12118.

Zeeshan, H., Lee, G., Kim, H.-R., and Chae, H.-J. (2016). Endoplasmic Reticulum Stress and Associated ROS. Int. J. Mol. Sci. *17*, 327.

Zhang, T., Xu, Y., Liu, Y., and Ye, Y. (2015). gp78 functions downstream of Hrd1 to promote degradation of misfolded proteins of the endoplasmic reticulum. Mol. Biol. Cell *26*, 4438–4450.

Strain & allele name	Mutation or transgene	Description	Strain source
Bristol N2	Wild type	Wild type animals, used to produce all other strains	Dahlberg Lab
sel-11 tm1743	473bp deletion, 38bp insertion	*hrd-1* putative null allele, large deletion, FJ861 is the backcrossed strain used	Caenorhabditis Genetics Center
VC35 *gk28*	1981bp deletion	*hrdl-1* putative null allele, large deletion, FJ863 is the backcrossed strain used	Caenorhabditis Genetics Center
VC20284 *gk121407*	W391stop	*marc-6* putative null allele, premature stop, CLD33 is backcrossed strain used	Million mutation project
VC20545 *gk146975*	T158I	*ubc-6* putative loss of function allele, nonconservative missense, CLD41 is backcrossed strain used	Million mutation project
VC40870 *gk857464*	P79L	*ubc-7* putative loss of function allele, nonconservative missense, CLD43 is backcrossed strain used	Million mutation project
CX32 *ky32*	*odr-10* null allele	results in loss of attraction of diacetyl	Caenorhabditis Genetics Center
CX3344 *kyIs53*	Podr-10::ODR-10::GFP	Wild type ODR-10::GFP	Caenorhabditis Genetics Center
CLD32	*kyIs53*; *tm1743*	*hrd-1* in Podr-10::ODR-10::GFP background	Dahlberg Lab
CLD31	*kyIs53*; *gk28*	*hrdl-1* in Podr-10::ODR-10::GFP background	Dahlberg Lab
CLD38	*kyIs53*; *gk121407*	*marc-6* in Podr-10::ODR-10::GFP background	Dahlberg Lab
CLD35	*kyIs53*; *gk146975*	*ubc-6* in Podr-10::ODR-10::GFP background	Dahlberg Lab
CLD42	*kyIs53*; *gk857464*	*ubc-7* in Podr-10::ODR-10::GFP background	Dahlberg Lab
CLD39	Podr-10::UBC-6::GFP	Transgenic strain used for UBC-6::GFP localization	Dahlberg Lab
CLD40	Podr-10::UBC-7::GFP	Transgenic strain used for UBC-7::GFP localization	Dahlberg Lab

Table 1. List of *C. elegans* strains used in our study. Strain and allele name provided with mutation/transgene, description of purpose in our study, and from where the strain was sourced.

Mutation detected	PCR step	Primer Name	Primer sequence
hrd-1	#1	tm1743 FWD	5’ GGTATCAGCTGGACTAATGATTGG 3’
		tm1743 REV	5’ GAACGGACGAACTGAGAAGAGTG 3’
hrdl-1	WT screen	hrdl-1 FWD	5’ GAGCCATCTGTAGAATATGGACAC 3’
		hrdl-1 REV	5’ GTGTGCCCGGACAATGCTTC 3’
	Mutant screen	hrdl-1 FWD	5’ GAGCCATCTGTAGAATATGGACAC 3’
		gk28 REV	5’ CGGGGAGCCGTTTGTGTCAATCC 3’
marc-6	#1	marc-6 exon FWD	5’ CGTGAAGAAGGTGAAGC 3’
		marc-6 exon REV	5’ CGATGACACTTAGGAACC 3’
	#2	marc-6 gk121407 FWD	5’ CTCCGCCCATTTTTCCGTGCCGC 3’
		marc-6 gk121407 REV	5’ CCAGACAATTTTCGTTACATGTGCG 3’
ubc-6	#1	UBC-6 MMP FWD	5’ GCAATACGCCCATTTCTGC 3’
		UBC-6 MMP REV	5’ CGTCCTGATGATGTTTCC 3’
		UBC-6 int MMP FWD	5’ CGTTGATTGGATTCCTGCC 3’
ubc-7	#1	UBC-7 MMP FWD	5’ GCTACTGGCACCTTCGTC 3’
		UBC-7 MMP REV	5’ CGAGTCCAACGCTTATGAGG 3’

Table 2. Primers used for detecting mutations in the E2 genes, *ubc*-6 and *ubc*-7, and E3 genes, *hrd-1*, *hrdl-1*, and *marc-6* when crossing mutations into the ODR-10::GFP background. **marc-6 genotyping requires sequential PCR amplification followed by restriction digestion by* Ear1.

Promoter Region:	Primer Name:	Primer designed:	Restriction Enzyme:
ubc-6	ubc6lprof (5' fwd)	(5') CCGGAAGCTTGCTGACTCTTCGATGG (3')	HindIII
	ubc6lpror (3' rev)	(5') CCGGGGATCCTTTATTCTCTAAATTCTCGTAC (3')	BamHI
ubc-7	ubc7prof (5' fwd)	(5') GATAAAGCTTTGGCAAGGTAAGAGC (3')	HindIII
	ubc7pror (3' rev)	(5') CCGGGGATCCCTATCTAGAAATAAATATAGAATTATCG (3')	BamHI

Table 3. Primers designed for amplifying the promoter regions of *ubc-6* and *ubc-7* oriented from 5' end to 3' end. Green highlighted regions indicate restriction enzyme site engineered into the primer for inserting the amplicon into an expression vector.

Coding Sequence:	Primer Name:	Primer designed:	Restriction Enzyme:
ubc-6	ubc6cs1f (5' fwd)	(5') CCGGGGTACCAAAAAATGAGTGAGCAGTAC (3')	KpnI
	ubc6cs1r (3' rev)	(5') GGCCGGTACCAACTCGGAACCG (3')	KpnI
ubc-7 (GFP downstream)	ubc7cs1f (5' fwd)	(5') CCGGGGTACCAAAAAATGGAGCAATCCTC (3')	KpnI
	ubc7cs1r (3' rev)	(5') GGCCGGTACCCATTCTTCTTGAC (3')	KpnI
ubc-7 (GFP upstream)	ubc7cs2f (5' fwd)	(5') CCGGGGTACCaaaaaATGGCGGCCGCgGAGCAATCCTC (3')	KpnI, NotI
	ubc7cs2r (3' rev)	(5') GGCCGGTACCTCATTCTTCTTGAC (3')	KpnI

Table 4. Primers used to amplify the coding sequence regions of *ubc-6* and *ubc-7* oriented from 5' end to 3' end. Green highlighted regions indicate restriction enzyme site KpnI incorporated into primer, purple highlighted region indicates NotI enzyme restriction site. Restriction sites were engineered to allow the amplified region to be inserted into an expression vector.

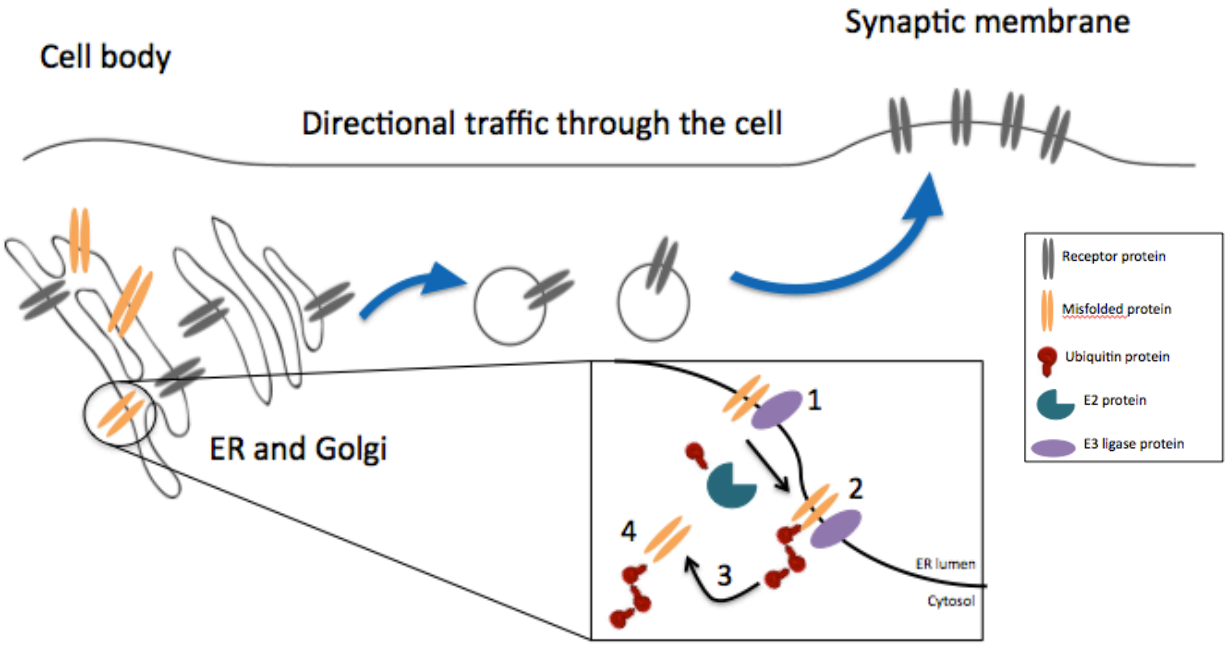

Figure 1. Model of ER-associated degradation (ERAD) in the neuron. 1) The E3 ligase targets and binds to the misfolded receptor protein. 2) The E2 ubiquitin carrying protein associates with the E3 ligase-receptor complex and polyubiquitinates the misfolded receptor. 3) The polyubiquitinated misfolded receptor is removed from the ER membrane into the cytosol. 4) The polyubiquitinated misfolded receptor is then targeted for degradation by the 26S proteasome in the cytosol.

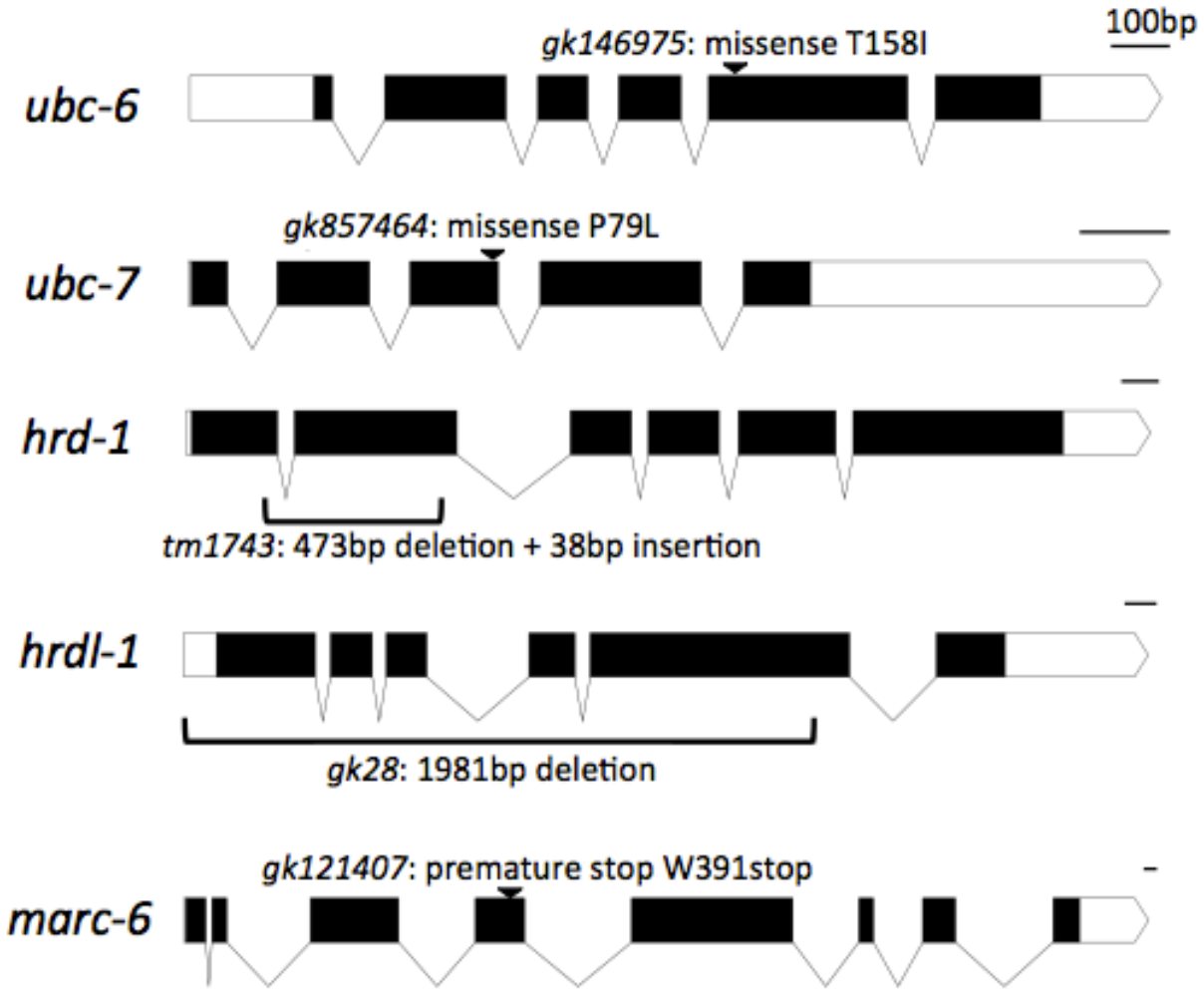

Figure 2. Schematic representations of gene structures and mutations resulting in putative loss-of-function mutations in the following E2 and E3 ligase mutant strains: *gk146975* (*ubc-6*), *gk857464* (*ubc-7*), *gk28* (*hrdl-1*), *tm1743* (*hrd-1*), and *gk121407* (*marc-6*). Brackets indicate deletions of gene sequences. *hrd-1* contains a deletion and subsequent insertion spanning exons 1-2, *hrdl-1* contains a deletion spanning exons 1-5, Arrowheads indicate where point mutations occur with respect to exons and introns within the gene sequence of the E2 and E3 ligase genes. *ubc-6* contains a nonconservative missense mutation T158I in exon 5, *ubc-7* contains a nonconservative missense mutation P79L in exon 3, and *marc-6* contains a premature stop at the end of exon 4, subsequently removing exons 5-8. Scale bar represents 100bp. Schematics were made using the Exon-Intron Graphic Maker found at www.wormweb.org.

```
S. cerevisiae      MA-----TKQAHKRLTKEYKLMVENPPPYILARPNEDNILEWHYIITGPADTPYKGGQYH      55
C. elegans         MSEQYNTKNAGVRRLMKEA-MELRQPTEMYHAQPMEDNLFEWHFTIRGTLGTDFEGGIYH      59
H. sapiens         METRYNLKSPAVKRLMKEA-AELKDPTDHYHAQPLEDNLFEWHFTVRGPPDSDFDGGVYH      59
                   *      .. . :** **    :.:*     *:* ***::***: : *  .: :.** **

S. cerevisiae      GTLTFPSDYPYKPPAIRMITPNGRFKPNTRLCLSMSDYHPDTWNPGWSVSTILNGLLSFM      115
C. elegans         GRIIFPADYPMKPPNLILLTPNGRFELNKKVCLSISGYHPETWLPSWSIRTALLALIGFL      119
H. sapiens         GRIVLPPEYPMKPPSIILLTANGRFEVGKKICLSISGHHPETWQPSWSIRTALLAIIGFM      119
                   * : :* :** *** : ::* ****: ..::***:*.:**:** *.**: * * .::.*:

S. cerevisiae      TSDE-ATTGSITTSDHHKKTLARNSISYNTFQN--VRFKLIFPEVVQE------------      160
C. elegans         PSTPGGALGSLDYPPKERQRLAKLSCEWKCKECGCVMKTALLPITEDGQLKQT-EEAKTL      178
H. sapiens         PTKGEGAIGSLDYTPEERRALAKKSQDFCCEGCGSAMKDVLLPLKSGSDSSQADQEAKEL      179
                    :   .: **:    ..:: **: * .:       .    ::*

S. cerevisiae      ------------NVETLEKRKLDEGDAANTGDETE---DPFTKAAKEKV-----------      194
C. elegans         AAQLKFQDESVVKKEVEAANNQKNPTETEPSEETSSVPTENVEESEE---------DADE      229
H. sapiens         ARQISFKAEVNSSGKTISESDLNHSFS--LTDLQDDIPTTFQGATASTSYGLQNSSAASF      237
                              . :.    . ..       :  .         : .

S. cerevisiae      ------ISLEEILDPEDRIRAEQALRQ-S------ENNSKKDGKEPNGSSSMVYIGIAIF      241
C. elegans         REEGTTVNVNSSEVPD--VAQPAVQPIRDPQPLVFQHHAPRLASTNFDYT-LLYK-IPVI      285
H. sapiens         HQPTQPVAKNTSMSPRQRRAQQQSQRRLSTSPDVIQGHQPRDNHTDHGGSAVLIV-ILTL      296
                         :  :    *             .      : :  :      . : ::   *  :

S. cerevisiae      LFLVGLFMK----------------------        250
C. elegans         ALCFAIFFT-LLARRFLVDNLTSPKDGSEL         314
H. sapiens         ALAALIFRRIYLANEYIFDFEL--------         318
                    :   :*
```

Figure 3. Amino acid sequence alignment of *C. elegans* UBC-6 in comparison to homologs *S. cerevisiae* (yeast) Ubc6 and *H. sapiens* (human) UBE2J1. Yellow highlighted threonine indicates missense mutation T158I in strain VC20545 *gk146975* located within the C-terminus helical bundle. The corresponding amino acid in H. sapiens is an aspartate and in *S. cerevisiae* is a lysine. Alignment performed using ClustalOmega.

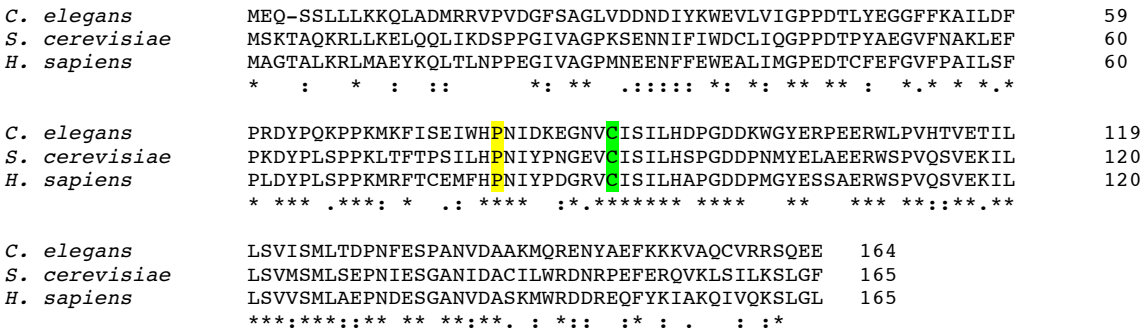

Figure 4. Amino acid sequence alignment of *C. elegans* UBC-7 in comparison to homologs *S. cerevisiae* (yeast) Ubc7 and *H. sapiens* (human) UBE2G2. Yellow highlighted proline indicates missense mutation P79L in strain VC40870 *gk857464* and indicates this proline is conserved across species. Green highlighted cysteine is the well-conserved catalytic cysteine in E2 proteins responsible for binding to ubiquitin. Alignment performed using ClustalOmega.

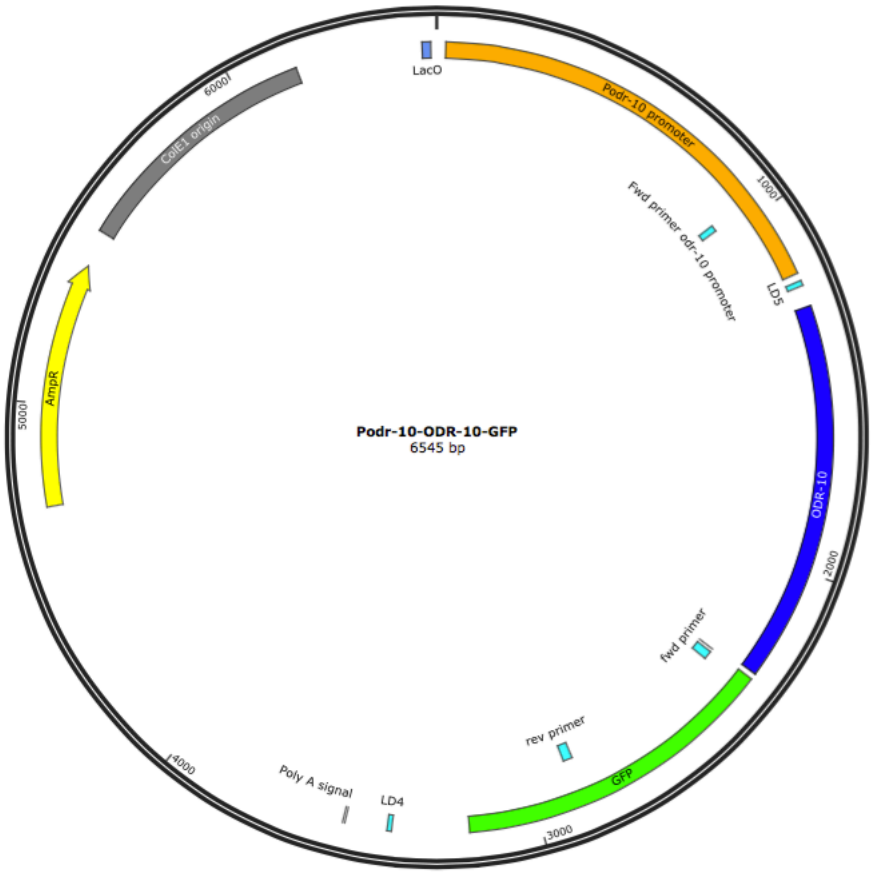

Primer Name:	Primer Sequence:
LD5 forward	(5') GGACCCAAAGGTAT (3')
LD4 reverse	(5') GGTGGGAGCACA (3')

Figure 5. Plasmid diagram of Podr-10::ODR-10::GFP. LD5 forward begins amplification just before the GFP coding sequence, and LD4 ends amplification just after the GFP coding sequence. Positive band size is 1168bp and indicates animals are carriers of ODR-10::GFP.

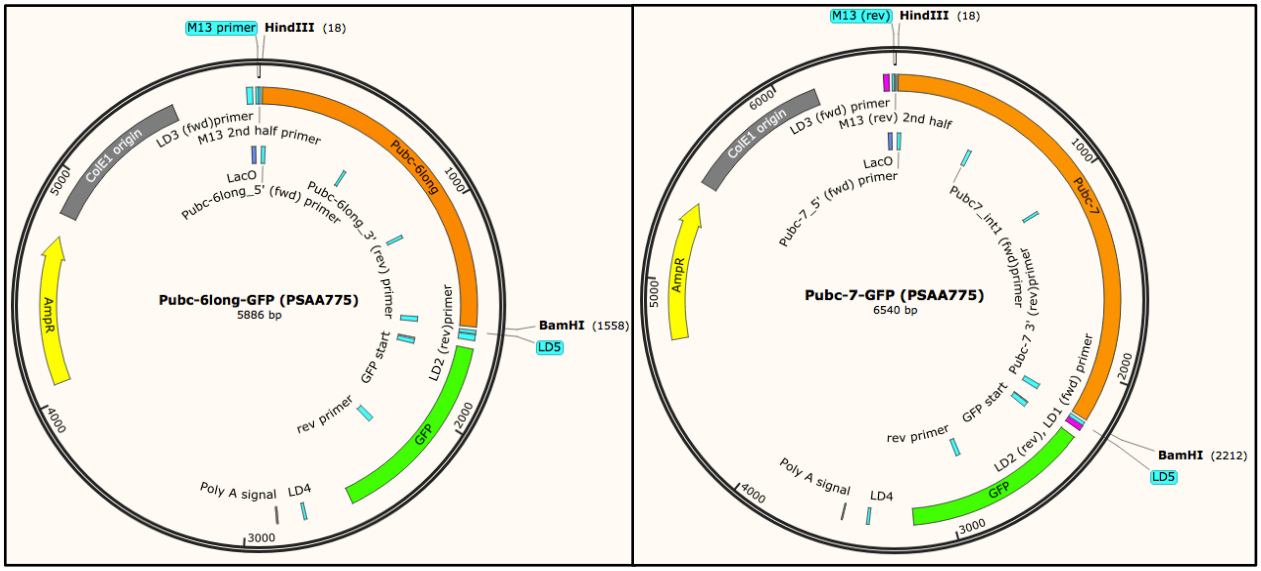

Figure 6. Plasmid maps of the E2 promoter reporter constructs P*ubc-6long*-GFP (left) and P*ubc-7*-GFP (right). The PSAA775 plasmid was used as the backbone for the creation of the constructs. Restriction digest sites used to incorporate promoter regions, BamHI and HindIII, are noted. The promoter regions are shown in orange; GFP is shown in green.

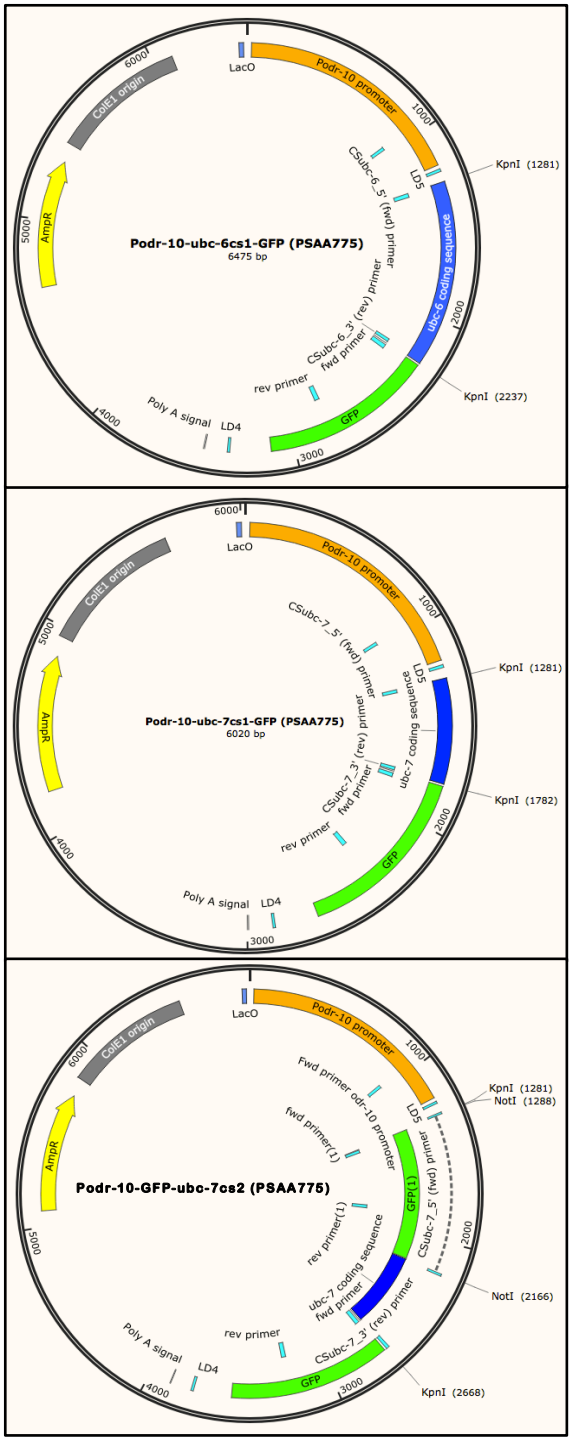

Figure 7. Plasmid maps of E2::GFP fusion reporter constructs inserted downstream of the *odr-10* promoter. P*odr-10-ubc-6cs1*-GFP (top), P*odr-10-ubc-7cs1*-GFP (middle), and P*odr-10*-GFP-*ubc-7cs2* (bottom). The PSAA775 plasmid if the backbone for these constructs. Restriction digest sites KpnI and NotI used for coding sequence insertion indicated on maps. GFP is in green and E2 coding sequences in dark blue.

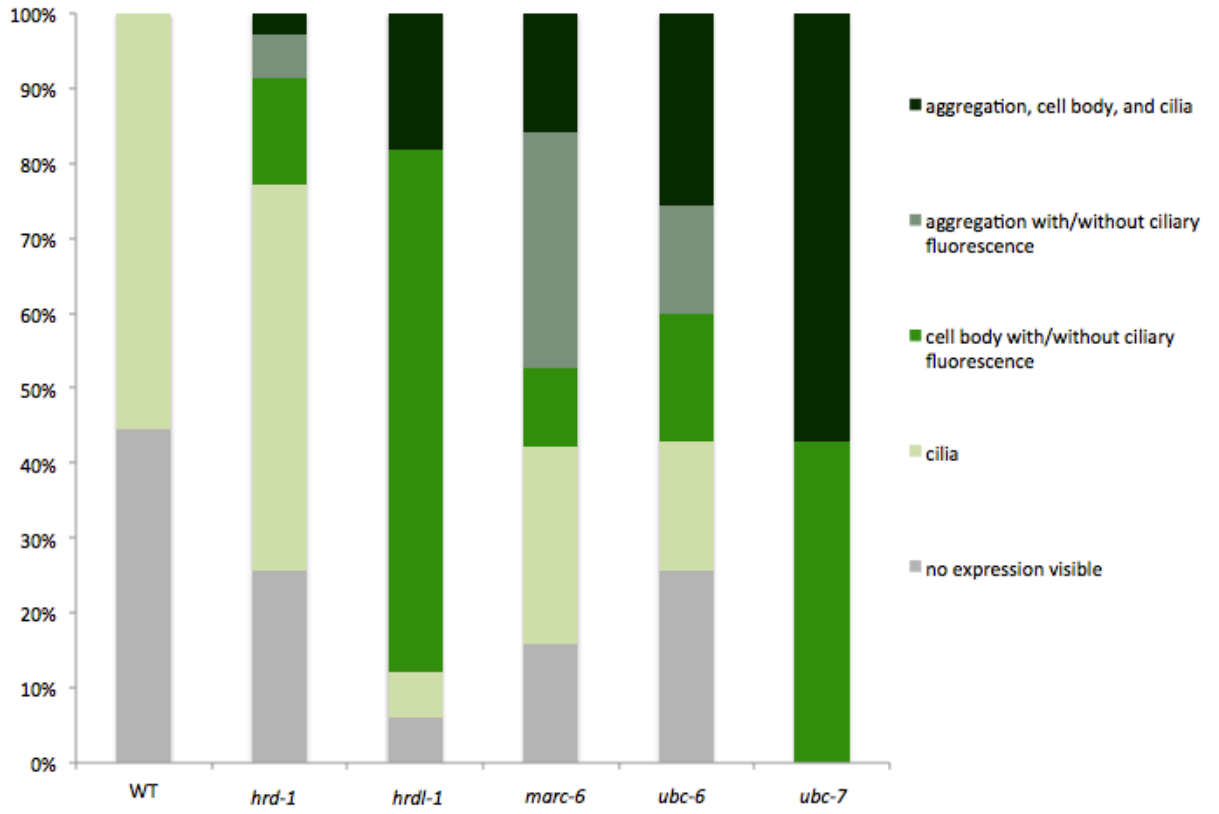

Figure 8. Quantitative data of ODR-10::GFP localization phenotypes observed in wild type (N=27), *hrd-1* (N=35), *hrdl-1* (N=33), *marc-6* (N=38), *ubc-6* (N=35), and *ubc-7* (N=28) mutants in the ODR-10::GFP background. Gravid adult worms were imaged and categorized by no visible fluorescence, ciliary fluorescence only, cell body fluorescence with or without ciliary fluorescence, aggregation in the neurite with or without ciliary fluorescence, and aggregation in the neurite with cell body and ciliary fluorescence.

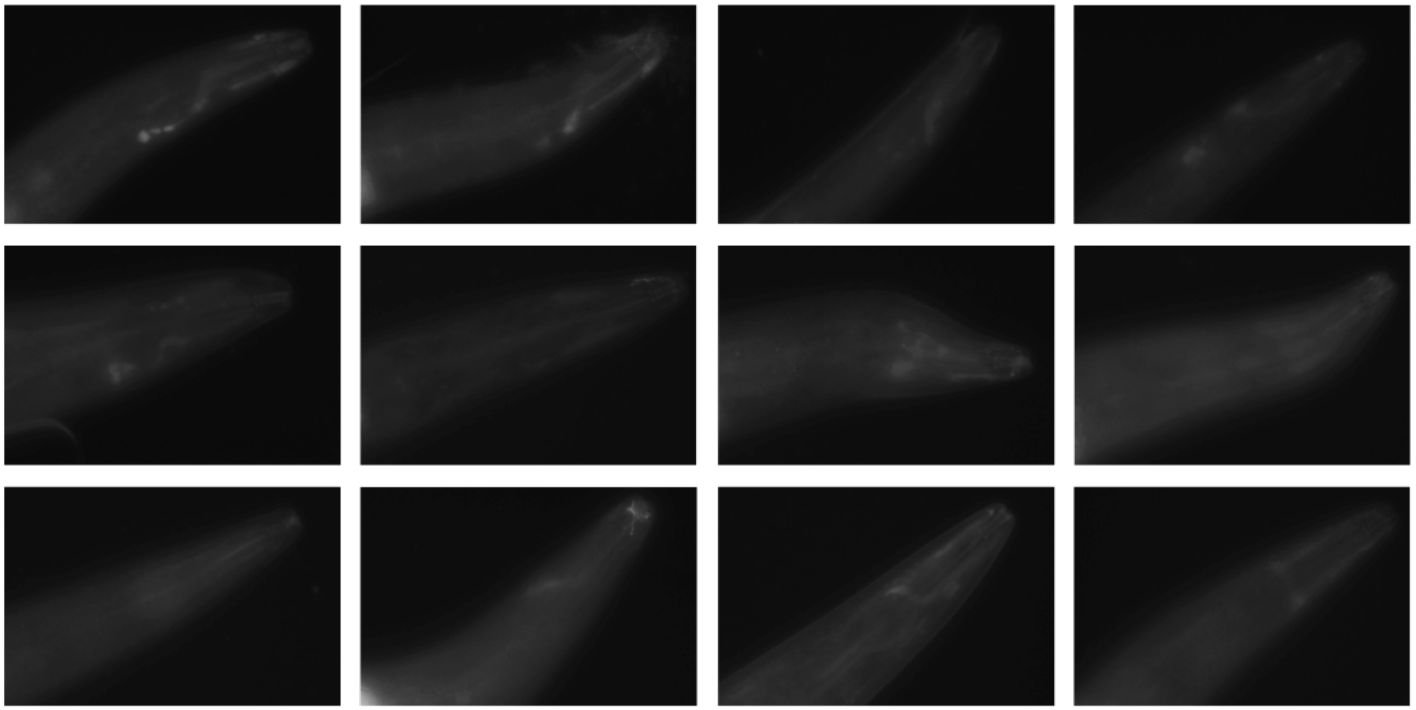

Figure 9. Representative images (n=12) of CX3344 *kyIs53* wild type gravid adult animals expressing ODR-10::GFP. Images taken on Leica DMi6000 at 400X total magnification. Contrast and brightness both adjusted to +20% (in PowerPoint) to enable fluorescence viewing. These are typical localization patterns observed in wild type animals where ODR-10::GFP expression is not frequent and if observed it is very dim.

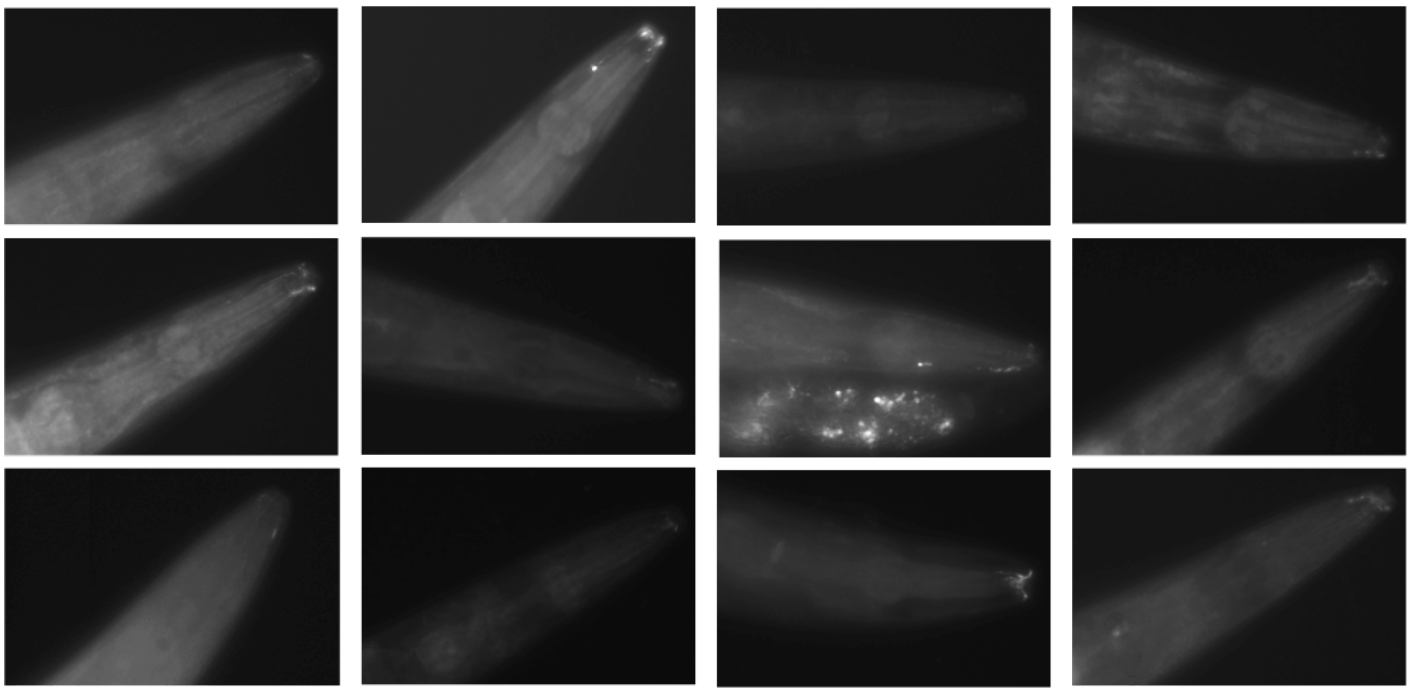

Figure 10. Representative images (n=12) of *hrd-1* mutant gravid adult animals in the ODR-10::GFP background. Images taken on Leica DMi6000 at 400X total magnification. Contrast and brightness are both adjusted to +20% (in PowerPoint) to enable fluorescence viewing. These are typical localization patterns observed under the *hrd-1* mutation.

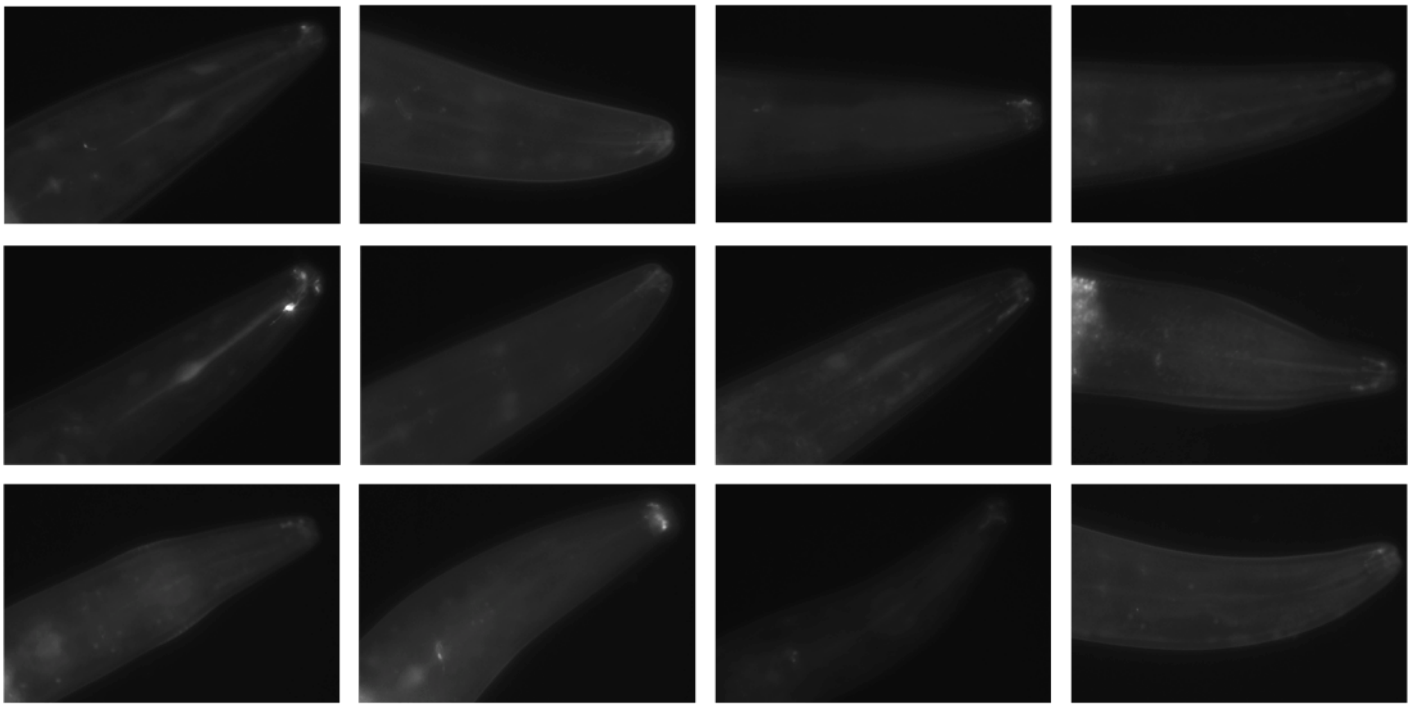

Figure 11. Representative images (n=12) of *hrdl-1* mutant gravid adult animals in the ODR-10::GFP background. Images taken on Leica DMi6000 at 400X total magnification. Contrast and brightness are both adjusted to +20% (in PowerPoint) to enable fluorescence viewing. These are typical localization patterns observed under the *hrdl-1* mutation.

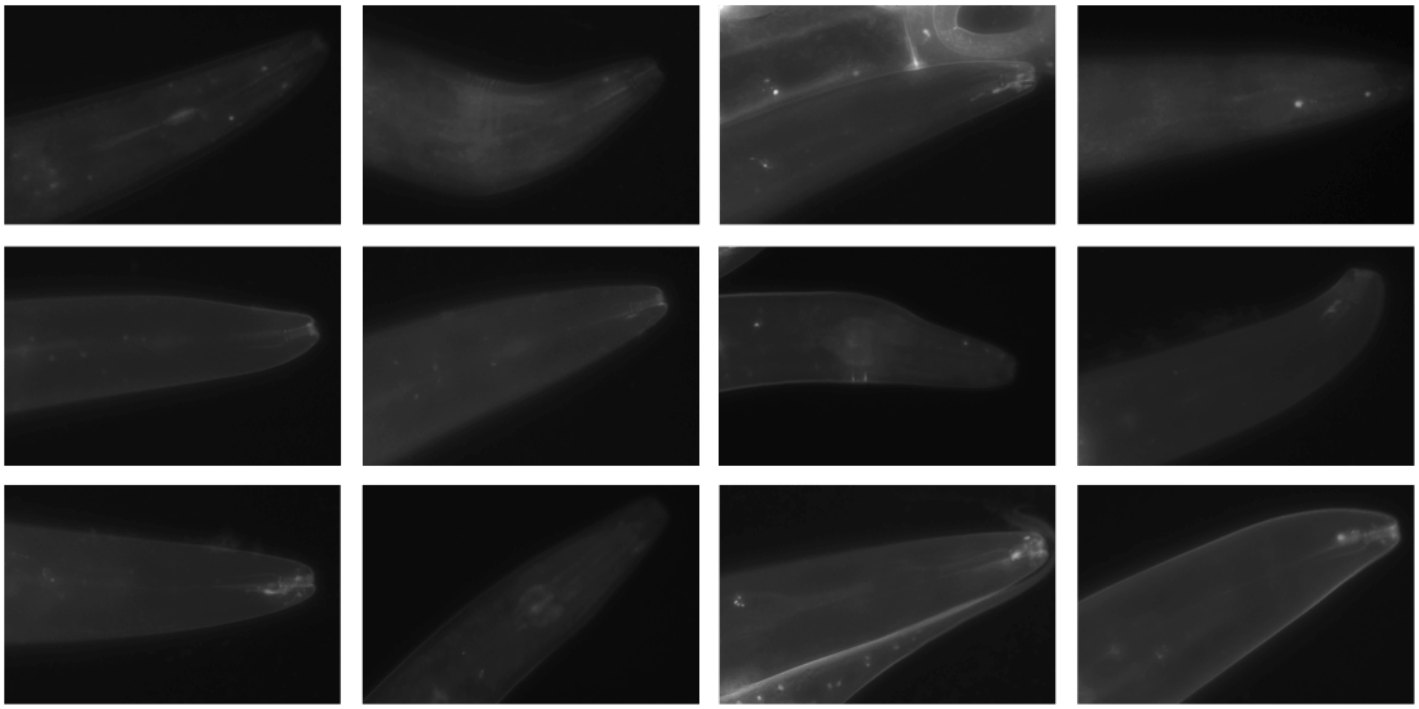

Figure 12. Representative images (n=12) of *marc-6* mutant gravid adult animals in the ODR-10::GFP background. Images taken on Leica DMi6000 at 400X total magnification. Contrast and brightness are both adjusted to +20% (in PowerPoint) to enable fluorescence viewing. These are typical localization patterns observed under the *marc-6* mutation.

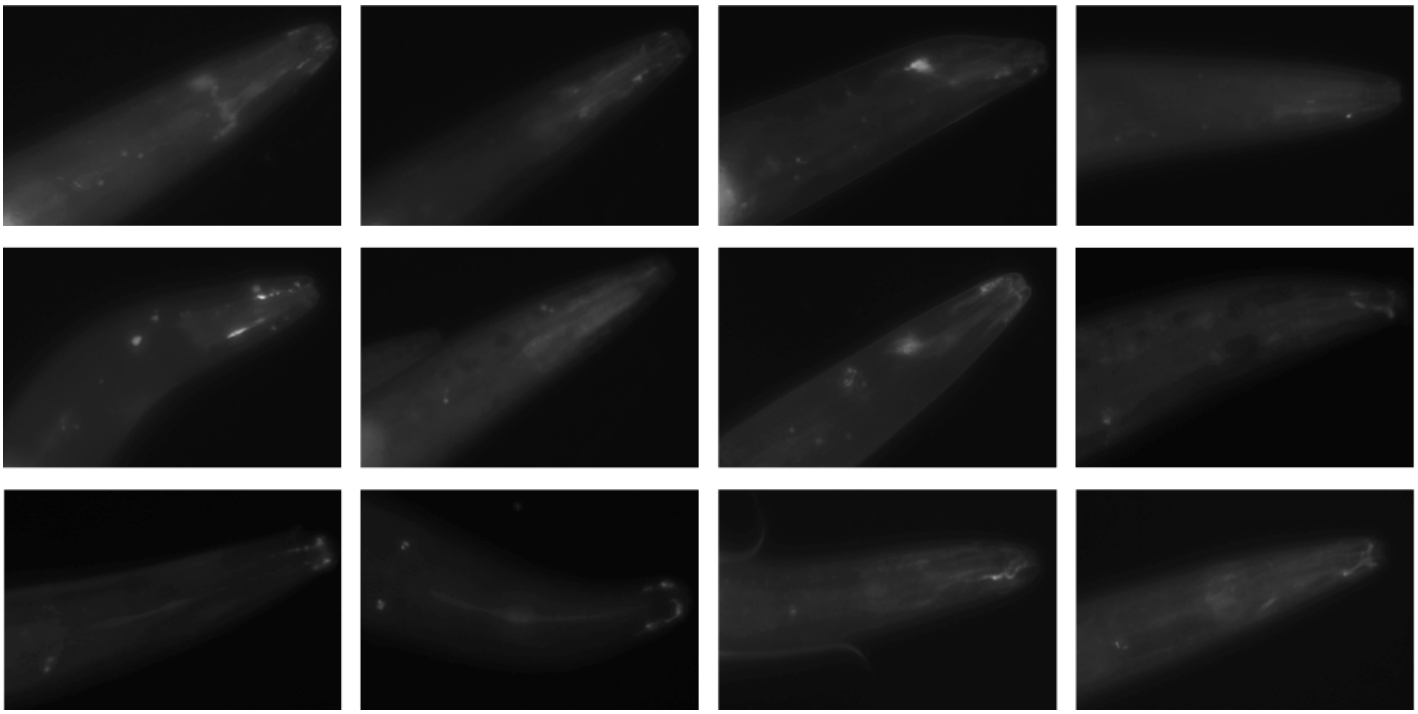

Figure 13. Representative images (n=12) of *ubc-6* mutant gravid adult animals in the ODR-10::GFP background. Images taken on Leica DMi6000 at 400X total magnification. Contrast and brightness are both adjusted to +20% (in PowerPoint) to enable fluorescence viewing. These are typical localization patterns observed under the *ubc-6* mutation.

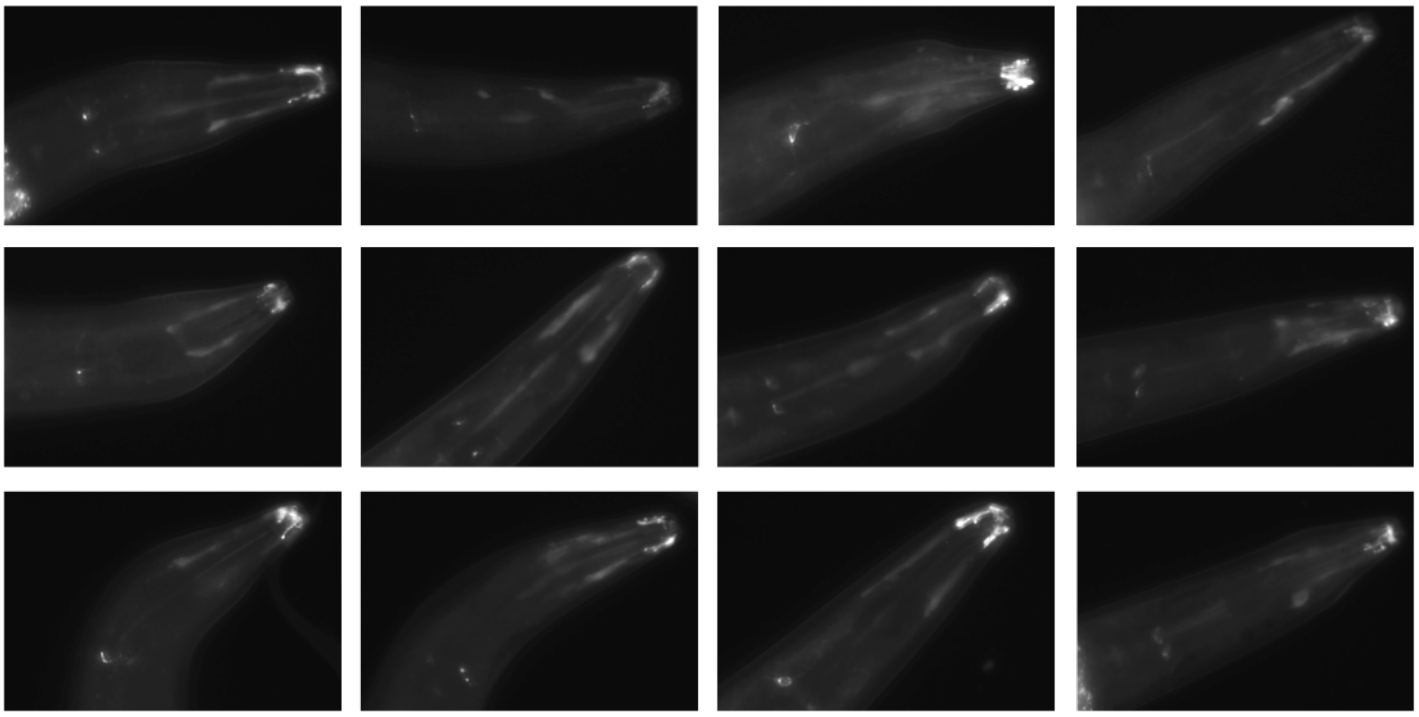

Figure 14. Representative images (n=12) of *ubc-7* mutant gravid adult animals in the ODR-10::GFP background. Images taken on Leica DMi6000 at 400X total magnification. Contrast and brightness are both adjusted to +20% (in PowerPoint) to enable fluorescence viewing. These are typical localization patterns observed under the *ubc-7* mutation.

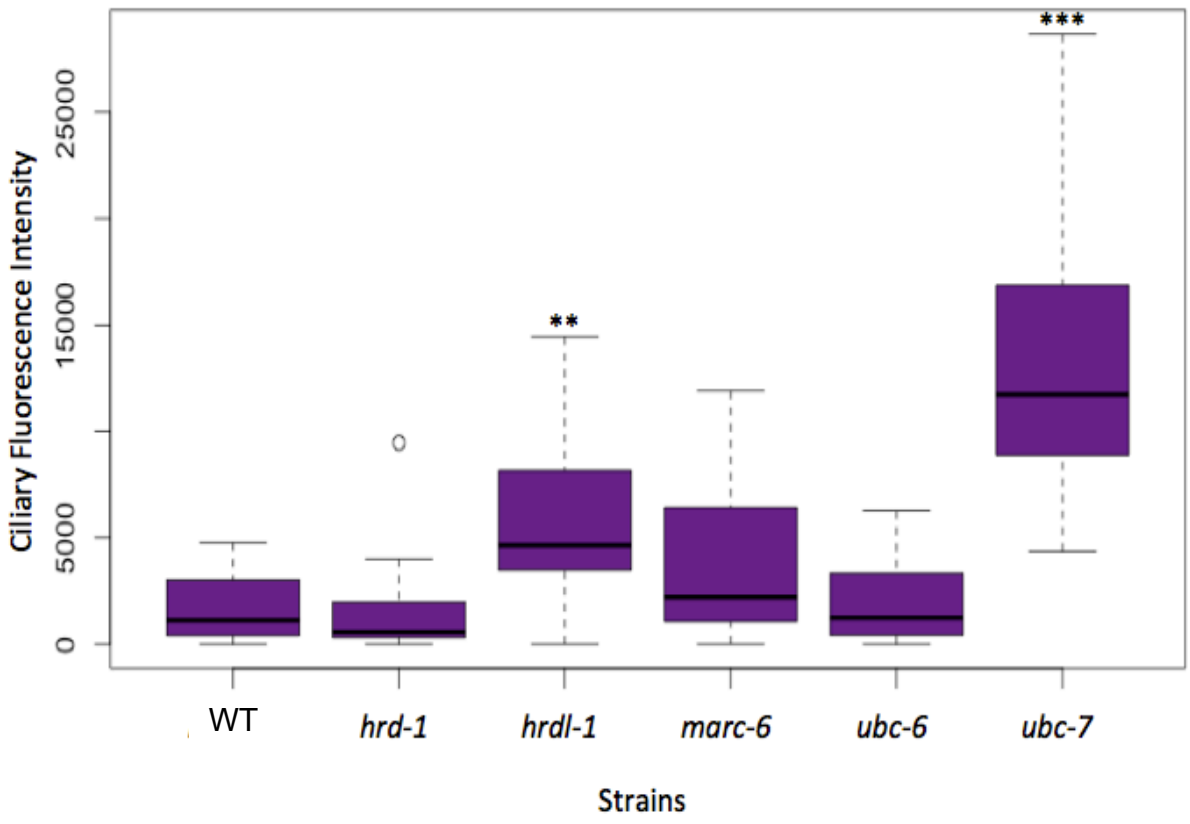

Figure 15. Box and whisker plot representing quantitative analysis of ciliary fluorescence intensity (arbitrary units) of animals in the ODR-10::GFP background. Strains analyzed were wild type (*kyIs53*), *hrd-1*, *hrdl-1, marc-6, ubc-6,* and *ubc-7.* 20 adult gravid worms were randomly selected and imaged per strain on the Leica DMi6000 and quantified via ImageJ analysis. If no fluorescence was visible the value given was 0 for that animal. White dots indicate outliers and error bars represent standard deviation. ** = $p<0.05$ and *** = $p<0.005$ in comparison to wild type with Tukey's HSD test.

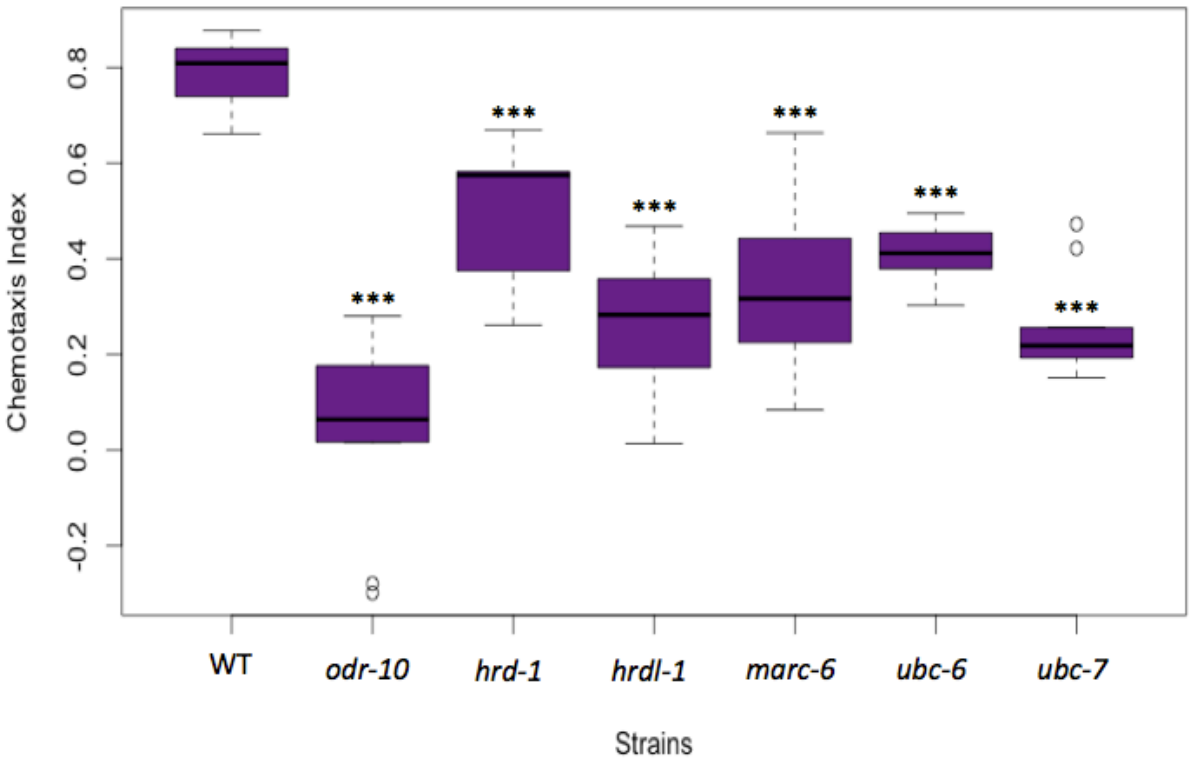

Figure 16. Box and whisker plot of chemotaxis index based on the behavioral phenotype for chemoattraction to diacetyl, the ligand for ODR-10. Negative control was 95% ethanol. White dots indicate outliers. Strains analyzed are wild type (n=17), *odr-10* knockout (n=11), *hrd-1 tm1743* (n=11), *hrdl-1 gk28* (n=10), and *marc-6 gk121047* (n=11), *ubc-6* (n=10), and *ubc-7* (n=10). *** = $p<0.005$ in comparison to wild type with Tukey's HSD test.

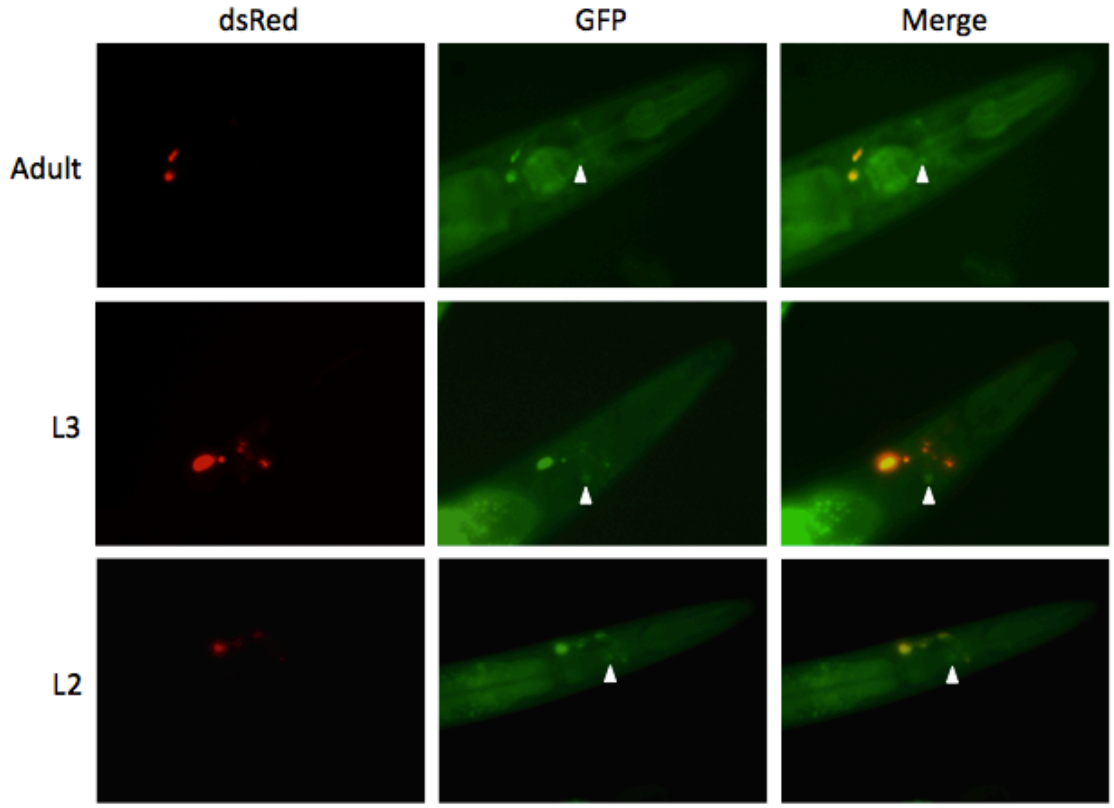

Figure 17. Fluorescent images of UBC-6::GFP transgenic animals at 400X total magnification. Images taken with a Leica DMi6000. P*ttx3*::dsRed was co-injected with the plasmid construct P*odr-10*::UBC-6::GFP as an injection control. GFP fluorescence indicates UBC-6 protein localization at the AWA cell body indicated by the white arrow. Images are merged to indicate cell body fluorescence is not dsRed. UBC-6::GFP fluorescence observed in animals at the adult, L3, and L2 stages in development. Brightness and contrast were adjusted in each image to enable viewing of cell body expression.

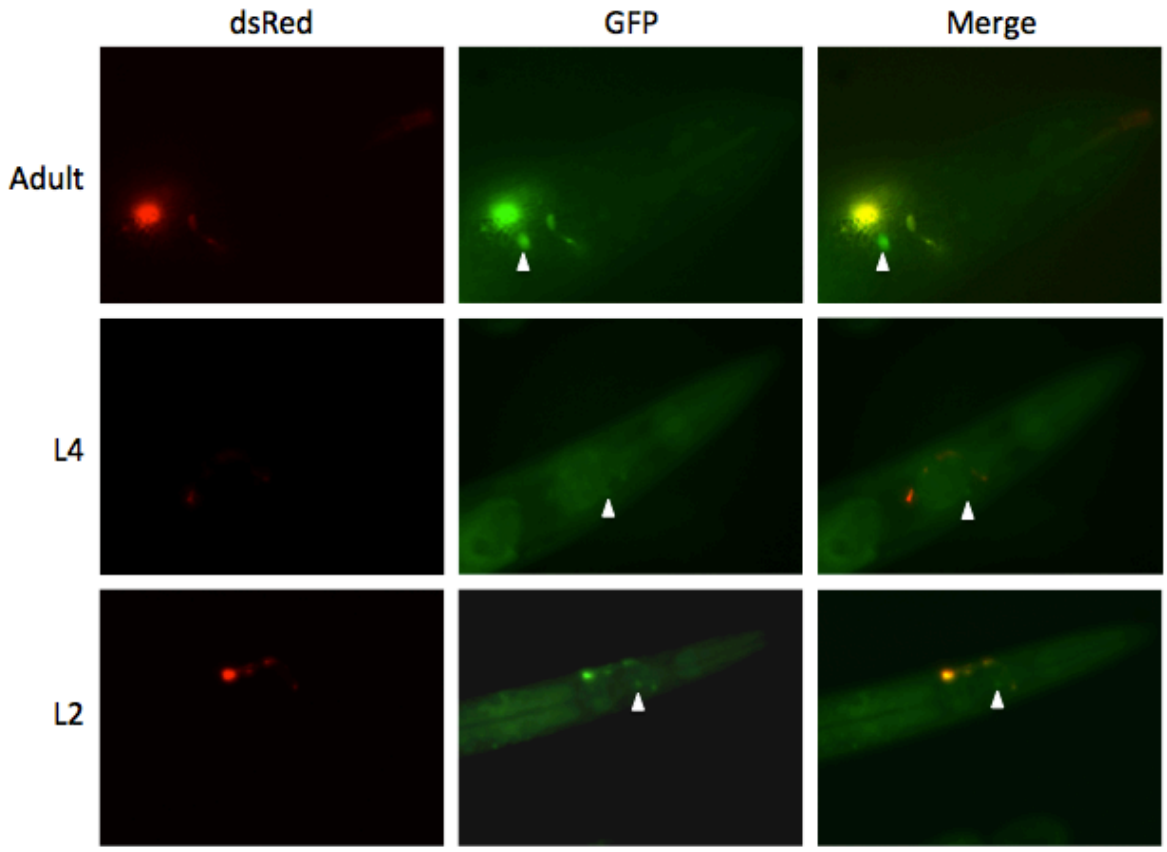

Figure 18. Fluorescent images of UBC-7::GFP transgenic animals at 400X total magnification. Images taken with a Leica DMi6000. P*ttx3*::dsRed was co-injected with the plasmid construct P*odr-10*::UBC-7::GFP as an injection control. GFP fluorescence indicates UBC-7 protein localization at the AWA cell body indicated by the white arrow. Images are merged to indicate cell body fluorescence is not dsRed. UBC-7::GFP fluorescence observed in animals at the adult, L4, and L2 stages in development. Brightness and contrast were adjusted in each image to enable viewing of cell body expression.

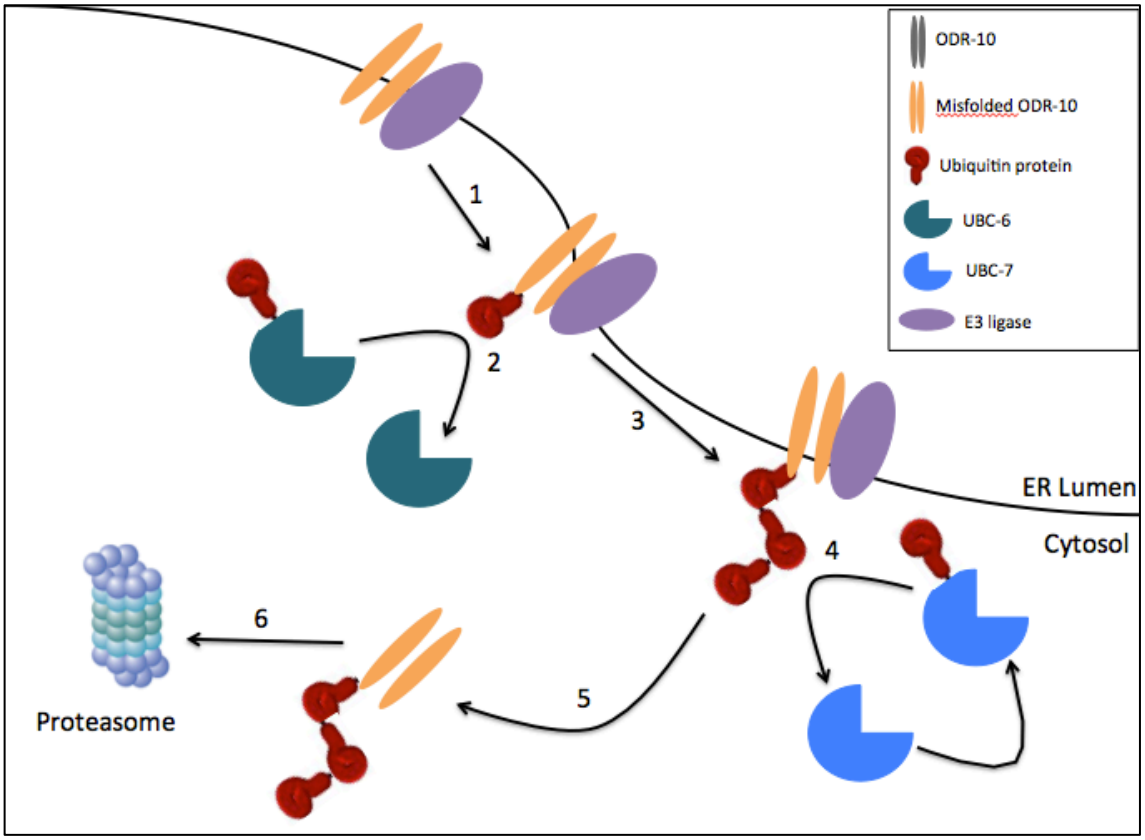

Figure 19. Our findings support a proposed ERAD ubiquitination model from yeast. 1) E3 ligase targets and binds to misfolded ODR-10 at the ER membrane. 2) UBC-6 primes the misfolded ODR-10 by adding one ubiquitin. UBC-7 is able to compensate for this role is UBC-6 is absent. 3) Once monoubiquitinated, UBC-7 adds another ubiquitin to the misfolded ODR-10. 4) UBC-7 will repeat this step creating a polyubiquitin chain until the necessary number of ubiquitins is attached for degradation signaling. 5) The polyubiquitinated misfolded ODR-10 is removed from the ER into the cytosol. 6) The 26S proteasome degrades the misfolded ODR-10 protein. (Weber et al., 2016)